University of Nevada, Reno

Observations of Hoppel Minima in CCN Spectra in Oklahoma

A thesis submitted in partial fulfillment of the
Requirements for the degree of Master of Science in
Atmospheric Science

By
Samantha S. Tabor

Dr. James G. Hudson/Thesis Advisor

August, 2015

THE GRADUATE SCHOOL

We recommend that the thesis
prepared under our supervision by

SAMANTHA SUZANNE TABOR

Entitled

Observations Of Hoppel Minima In CCN Spectra In Oklahoma

be accepted in partial fulfillment of the
requirements for the degree of

MASTER OF SCIENCE

James G. Hudson, Ph.D., Advisor

David Mitchell, Ph.D., Committee Member

Mario Alpuche, Ph.D., Graduate School Representative

David W. Zeh, Ph.D., Dean, Graduate School

August, 2015

Abstract

Aerosols are one of the most fundamental keys to understanding the future state of the climate. Aerosols impact the radiation budget of the Earth in numerous ways and are poorly understood. Some aerosols can act as cloud condensation nuclei (CCN) and can significantly change the properties of clouds; this is known as the Indirect Aerosol Effect (IAE) and it remains the largest climate change uncertainty. Most studies concerning CCN and the impacts of the CCN distributions occur over the ocean, leaving questions about the processing occurring over the continents. Eleven days of measurements from the Atmospheric Radiation Measurement (ARM) Southern Great Plains (SGP) site were taken from an Aerosol Intensive Operational Period (IOP) during May 2003. A ground based CCN spectrometer and differential mobility analyzer (DMA) were deployed to study the distributions of the CCN spectra and dry aerosol size distributions. 268 measurement periods were sorted by their spectral shapes by using two rating systems. Case studies of the characteristics of the spectra observed during specific times of day or particular meteorological conditions were created and it was shown that meteorological conditions have a significant impact on the shapes of the CCN distributions. Back trajectories were also analyzed and shown to have an even larger impact on the observations of the Hoppel Minima, a minima located between the processed and unprocessed CCN modes. Using vertical velocity and back trajectories along with numerous meteorological measurements it can be shown that cloud processing is not only occurring over the continent but transport of the cloud processed air to the

surface is also occurring. The Hoppel Minima during this Oklahoma project had a mean critical supersaturation (S_c) of 0.68%.

Dedication

For God, Mom and Dad, Tabitha, Jeremy, and Guinevere for always being there for me and for cheering for me all along the way!

Acknowledgments

Data were obtained from the Atmospheric Radiation Measurement (ARM) Program sponsored by the U.S. Department of Energy, Office of Science, Office of Biological and Environmental Research, Climate and Environmental Sciences Division. Satellite and surface observation data were obtained from the University Corporation for Atmospheric Research (UCAR) Mesoscale and Microscale Meteorology Laboratory (MMML). Radar data were provided by the National Climate Data Center. The DMA data were provided by Dr. J. Wang.

Contents

List of Tables

List of Figures

Introduction

The effects of aerosols on radiative forcing (RF) still remain the largest source of uncertainty in the global RF estimate (*Alexander et al., 2013*). Some aerosol particles can act as cloud condensation nuclei (CCN) which can lead to significant impacts on various cloud properties, known as the Indirect Aerosol Effect (IAE). Aerosols can alter cloud albedo, causing brightening, and can alter precipitation, which can impact cloud lifetime and thus global albedo (*Albrecht, 1989; Platnick and Twomey, 1994*). This phenomenon was first noted by Twomey (1976, 1977), who saw that pollution influenced the albedo of clouds which altered the planetary albedo. Over the ocean in a relatively clean environment, clouds are more susceptible to aerosol changes, which contributes to their global RF cooling effect (*Carslaw et al., 2013*). Numerous studies conducted over the ocean have also been used to study the properties of aerosols and CCN in the marine boundary layer (MBL), such as during the Marine Stratus/Stratocumulus Experiment (MASE; July 2005) and Ice in Clouds Experiment-Tropical (ICE-T; July 2011) (*Hudson and Noble 2014a, 2014b; Hudson et al. 2015)*.

During numerous studies of aerosol spectra over the ocean, a double peaked feature, now known as the Hoppel Minimum, was often seen in the aerosol spectra. Hoppel et al. (*1985, 1986*) first noted the phenomenon during marine research cruises and attributed it to in-cloud processing. The main mechanism behind the processing was concluded to be non-precipitating cloud cycles (*Hoppel, et al. 1985*). During each cloud cycle, larger aerosols (that is, particles with a low critical supersaturation S_c) become activated into cloud droplets. The modality of the spectra, which can range from strictly

monomodal to very bimodal, is thought to be a result of both physical and chemical processing occurring in the clouds (*Hudson et al., 2015*). Each can lead to a double peaked (bimodal) spectrum.

Hoppel et al. (*1985*) proposed four possible mechanisms that could be causing the frequently seen double peaked feature. Three of the mechanisms were dismissed and it was proposed that chemical formation due to absorption of gases by droplets during cloud cycles could cause a minimum to appear in the size distribution spectrum. This is what is referred to as chemical processing. Mass can be added to the CCN through heterogeneous chemical processes; for example, the chemical transformation of sulfur dioxide (SO_2) through the conversion of S(IV) to S(VI) is widely studied (Feingold, 2000).

Physical processing has also been shown to have importance in the formation of a bimodal size distribution of CCN (*Hudson et al. 2015*). Activated cloud droplets collide and coalesce, causing two CCN to form into one new aerosol mass. Thus, when the cloud evaporates the resulting aerosol (known as the processed aerosol), has become larger than it was before activating. Brownian capture of cloud interstitial material, a physical process, can also contribute to bimodal spectra (*Hudson et al. 2015*). Determination of the type of cloud processing can be investigated from the change in the CCN number concentration (N_{CCN}) and cloud droplet concentration (N_c) before and after processing. In both scenarios, the critical supersaturation (S_c) would be reduced due to the increasing size of the CCN. Chemical processing should not alter N_{CCN}, as it is only adding mass to

the already existing CCN, and physical processing would reduce N_{CCN}, due to the collision and coalescence of droplets containing activated CCN.

Cloud processing is thought to continue for up to ten cycles (*Pruppacher and Klett 1978; Hoppel 1986*) and results in the formation of Hoppel minima between the processed and unprocessed particles. Because the minima forms as a result of differences between activated and unactivated CCN, the location of the minima can then be used to infer the supersaturation of nearby clouds (*Hoppel et al., 1985, 1986, 1994; Clarke et al. 1996, 1998, 1999, 2004, 2013*). This method will be discussed in later sections.

Cloud processing and its effects on aerosols and clouds have been studied by Twomey (*1974, 1977*), Feingold et al. (*1996, 1998*), Zhang et al. (*1999*), and Feingold and Kreidenweis (*2000*) as well as the bimodal result of cloud processing (*Hoppel et al. 1986, 1990, 1994, 1996; Hudson et al. 2015*) however the majority of these studies were conducted either over the ocean or near coastlines. While there have been studies of aerosols over the continent (e.g *Svenningsson et al. 1997*; *Swietlicki et al.* 1999; *Zhou et al. 2002*), few CCN-centered studies have occurred over or in continental environments (e.g. *Roberts et al. 2001; Bougiatioti et al. 2011*). Of these few studies, none focused on the modality of the CCN distributions.

In this study, in-situ measurements were performed at the Atmospheric Radiation Measurement (ARM) Southern Great Plains (SGP) Climate Research Facility during the Aerosol Intensive Operational Period (IOP) Field Campaign that occurred from May 5-31, 2003. Using a ground-based CCN Spectrometer (*Hudson 1989*). Measurements of CCN (aerosols activated into cloud droplets using a cloud chamber) were made alongside

a differential mobility analyzer (DMA) measuring the dry aerosol. The size distributions obtained from the DMA were then fitted to the CCN spectra from the spectrometer in order to determine the best fit kappa (κ) value (*Petters and Kreidenweis, 2007*) for the sample aerosol. Assigning κ value to the sample yields the hygroscopicity of the sample as well as evidence of chemical processing; for example, if κ values are different for the processed and unprocessed peaks of the spectra, then it is possible that the hygroscopic value of the aerosol changed during processing. From here, S and S_c can be determined using Petters and Kreidenweis' (*2007*) κ-Köhler theory.

From the spectrometer data, $\frac{dN}{dlogS_c}$ can be calculated, where N is the CCN number concentration in cm^{-3} and S_c is the critical supersaturation. This was then plotted against S_c (from 0.01% to 2%) to create the CCN distributions. The distributions can then be categorized into one of eight modal ratings, from purely bimodal (one) to purely monomodal (eight) (*Hudson et al. 2015*) (Figure 1; all figures can be found in the Figures section, beginning on page 38). Seeing how the modal ratings change with time is important to understand if there is cloud processing occurring and on what time scale these changes are happening.

The CCN distribution plots were then used alongside radiation, air trajectory analysis, satellite measurements and surface observations in order to determine the following:

1. Can the Hoppel Minimum be identified in the spectrometer data?
2. Is cloud processing occurring over the continent; specifically, over the Southern Great Plains?

3. If so, what conditions lead to the formation of the Hoppel Minima when compared to days with no Hoppel Minima present?

These questions will be addressed in subsequent sections.

Methods

Overview

Eleven days of data were evaluated between May 11-26, 2003 at the Atmospheric Radiation Measurement (ARM) Southern Great Plains (SGP) Climate Research Facility, located near Lamont, Oklahoma (which is 85 miles north of Oklahoma City), as a part of the month-long Aerosol IOP Field Campaign. Two Desert Research Institute (DRI) CCN spectrometers (*Hudson* 1989) were located on the ground and were running nearly continuously from May 5 to May 31. The spectrometers were calibrated using an electrostatic classifier (EC, also referred to as a DMA) to obtain a monodisperse aerosol of known composition to have the spectrometers sample and therefore obtain a relationship between S_c and channel number. Individual time periods were selected where the mean number concentration of CCN (N_{CCN}) was not changing greatly (that is, no more than approximately 10% variation during each period) and not during calibration periods. The average duration and standard deviation of the selected periods can be seen in Table 1 (all tables can be found in the Tables section, beginning on page 32). These time periods were then used to plot the average CCN distributions. DMA size distributions were then fitted to the CCN data using a hygroscopicity value (κ) and then rated according to their modality on a scale of 1 to 8, where 1 is purely bimodal and 8 is purely monomodal (*Hudson et al. 2015*). S_c of both the processed and unprocessed modes

and the Hoppel Minimum is recorded. N_{CCN} of both modes is also recorded, including the maxima, minima, and total integrated concentrations. Differences between the processed and unprocessed S_c and N_{CCN} when combined with κ can yield information regarding the amount and type of processing. These differences, noted as S_u-S_p (the difference between unprocessed and processed S_c) and N_u-N_p (the difference between unprocessed and processed N_{CCN}), can be plotted against different parameters such as time of day which could yield correlations leading to hypothesizing the origins of bimodal CCN spectra.

Similarly to S_u-S_p and N_u-N_p, the modal ratings of each time period are plotted against the hour of the day in order to show the changes in the CCN spectra with time. These changes with time can then be related to solar radiation measurements and satellite imagery in order to determine the presence of clouds in the area. Air trajectory analysis was used to determine if there is anything of significance upwind of the sampling site, such as passage over heavily polluted areas. Satellite imagery coupled with air trajectory analysis may also give insight to whether or not clouds are forming and dissipating upwind, yielding evidence of cloud processing.

Calibration Methods

During the IOP, the CCN spectrometers were calibrated at least twice daily. The need for periodic calibration is three-fold, as noted by *Hudson* (1989): first, to check the entire system as a whole; second, to check the condensation coefficient; and third, to recalibrate the spectrometer if the parameters have shifted or needing adjustment. It has since been shown, however, that the condensation coefficient is constant (*Raatikainen et al. 2013*).

The calibration process was similar to that described by *Hudson* (*1989*, *2007*). As in previous studies, monodisperse, soluble salts with known S_c (*Gerber et al. 1977*) were aerosolized and then sampled by the spectrometer in order to produce a monodisperse droplet spectrum that can then be associated with the S_c of the aerosol. A salt solution generally consisting of sodium chloride (NaCl) but occasionally ammonium sulfate ($(NH_4)_2SO_4$) was aerosolized and run through an electrostatic classifier (EC, also known as a DMA). The EC causes a monodispersion of the aerosol to be produced, which is then sent to the spectrometer. This resulted in monomodal droplet distributions which are plotted against channel number to make a calibration curve. This curve provides a relationship between the known S_c of the initial aerosol input and the channel number. Knowing this relationship, a S_c spectrum can be determined during sampling periods (*Hudson 2007*).

The DMA was operated alongside a condensation particle counter to form a Scanning Mobility Particle Sizer (SMPS). The SMPS was calibrated using polystyrene latex standards (*Wang et al. 2007*). For a more detailed explanation of the SMPS, *Wang et al.* (2003) can be consulted. Figure 2 shows the relationship between the total number concentrations obtained by the DMA versus the CCN spectrometer, up to 2% S_c. This correlation, with R = 0.79 and a significance level (SL) of 100%, verifies that the CCN spectrometer is working correctly relative to the DMA.

Spectrometer Measurements

The spectrometers were taking measurements (referred to as duct mode) almost continuously during observation periods and were calibrated, which was described in the

previous section and by *Hudson* (1989). These observation periods were coordinated to line up with research flights that were also a part of the ARM 2003 IOP (*Wang et al. 2007*). This caused variability in the time of day of the measurements, with some days having samples during morning, midday, afternoon, late evening (post sundown) or even all twenty-four hours of the day.

The DRI CCN Spectrometer measurements depend highly on the calibration system described earlier in order to assign S_c to the dry CCN that have been sampled. During the duct mode, ambient air is moved into a cloud chamber which condenses water vapor onto the particles to form droplets. The droplets grow as they travel along a path with increasing S. The droplets are then measured by an optical particle counter (OPC), yielding a drop size distribution, which can then be used with the S_c-channel number relationship to calculate the dry aerosol S_c against CCN concentration (*Gerber et al. 1977*).

These calculated spectra are then averaged over periods ranging from 1 to 144 minutes (average of 25 minutes; Table 1). The average percent N_{CCN} variation within each of the eleven days can be seen in Table 2. The peaks and minima in the spectra are recorded to determine differences between the unprocessed and processed modes as well as how the shape of the spectra changes with time. Finally, the derived spectra are then rated on a 1-8 scale based on their modality and then compared to various parameters such as solar radiation measurements; both will be discussed in the upcoming subsections.

Modal Ratings

In order to understand and compare the features of the CCN spectra, the modality should be quantified. This is done by using a 1 to 8 modal rating scale (*Hudson, et al.* 2015). Eight categories are used because often the modes are not well separated (Fig. 1a versus Fig. 1d) or possess features that distinguish the spectra from either a pure bimodal or monomodal category. The rating system ranges from purely bimodal (Fig. 1a) to purely monomodal (Fig. 1h) and depends on subjective judgement. Each spectra was closely examined and rated subjectively as it has been shown previously that quantifying overlapping modes with computer software, such as PEAKFIT, was unsuccessful (*Hudson et al. 2015*). It is important to remember that the modal ratings quantify the scale of modality; that is to say, the spectra in question is more bimodal (ratings 1-4) or monomodal (ratings 5-8). The modal rating system does not necessarily quantify the amount of processing. For example, a purely monomodal spectra, rated an 8, can be located in an area of lower S_c, which would imply processed CCN, or located in an area of higher S_c, implying unprocessed CCN.

In addition to observing the daily changes in modal ratings, all of the modal ratings were separated into seven time periods in order to see if time of day influenced spectral modality. These time periods included Day (measurements and ratings during the hours of 0600-2100 local time) and Night (2100-0600), as well as five sub time periods: Morning (0500-1000), Midday (1000-1500), Afternoon (1500-2000), Evening (2000-2400/0000), and Late Night (0000-0500). Modal ratings were also compared within four

specific case types in order to see the effect of daily meteorology: sunny, overcast mornings, partly cloudy, and overcast.

A supplement to the modal rating system of Hudson et al. (*2015*) was also created for the purposes of this paper. A supersaturation, noted as S^*, is chosen as the distinction between unprocessed and processed CCN. These modes can be characterized by the difference between the peak processed supersaturation S_P and the peak unprocessed supersaturation S_U as well as the difference between the processed number concentration N_P and unprocessed number concentration N_U. The signs of N_U-N_P (the difference between the integrated unprocessed peak and processed peak) and S_U-S_P (the difference between the locations of the unprocessed and processed peaks) are evaluated to determine the amount of processing and distance between the modes respectively. The spectra can also sorted into monomodal and or bimodal by noting if S_M could be estimated. If no Hoppel Minimum can be determined, the spectra can then be sorted by comparing the monomodal peak supersaturation S_M to S^*; if S_M is greater than S^* it is labeled "I" (Fig. 3a) and if it is smaller it is "VI" (Fig. 3e). Spectra rated "VI" may seem contradictory and it doesn't necessarily represent spectra that are truly cloud processed and monomodal; it simply describes monomodal spectra with a peak S_c less than the chosen S^*.

If S_U is smaller than S^*, the spectra is rated "V"; but this rating was not observed in this project. If S_P is greater than S^*, it is labeled "II" (Fig. 3b) and has both modes located in the processed half of the S_C scale. If S_P is smaller than S^* while S_U remains larger, N_U- N_P is then used to determine which mode is larger. When N_U- N_P is negative the spectra is "IV" (Fig. 3d) and when N_U- N_P is positive the spectra is "III" (Fig. 3c). It

is important to note that both “III” and “IV” are both bimodal with the processed peak lying to the left of S^* and the unprocessed peak to the right; that is, while a spectrum may be labeled as “III,” it is not stating that the air represented in the spectra has not been processed and vice versa for “IV”. It is simply stating the dominant mode of the spectra.

This unprocessed/processed rating system, hereafter referred to as the U/P rating, is complimentary to the primary modal rating system as it describes the amount of processing. The primary modal rating does not always discriminate between spectra that are completely processed ($S_{U/M} < S^*$) or unprocessed ($S_{P/M} > S^*$) unless directly altered by those determining the modal rating of each individual spectra. By combining the two systems we can not only accurately describe the shape and location of the spectra. It may even be possible to determine factors that have influenced the spectra as well as the amount of processing that has occurred by determining a best fit S^* for the dataset. For this paper, S^* was selected to be 0.3% as it is an average location of the Hoppel Minima in previous studies (*Hudson et al. 2015*).

Solar Radiation Measurements

These measurements were obtained from a pyranometer and will be combined with satellite data, described below, in order to determine the presence of clouds during the analysis period by comparing days with continuous and interrupted measurements (Fig 4). On days with interrupted radiation (Fig 4b), it will be presumed that clouds were present and that cloud processing may therefore be occurring in the area. These results will be combined with other measurements, such as satellite and surface analysis, in order to understand a complete picture of the surrounding environment.

In order to compare cloudy days to sunny days, a standard sunny day case should be selected from the available data. May 5, 2003 was chosen as the set sunny day for comparison with the eleven observation days selected from the study. A percentage of total available incoming shortwave radiation was calculated by matching the closest measurements on each day and determining the ratio for the observation day compared to the sunny day. The sunrise and sunset times between the first and last observation day were approximately 10 minutes apart and approximately 5-15 minutes apart from the sunny day, leading to only minor differences in percentage calculations in the early morning and late evening hours.

Air Trajectory Analysis Methods

Back trajectories have been used extensively in previous studies of CCN and related aerosols (*Hoppel et al. 1985, 1986, 1990, 1996*; *Dusek et al. 2009; Holmgren et al. 2014; Yakobi-Hancock et al. 2014*) as they give information as to where the air in question has originated and where it has passed over. Air trajectory analysis was done using the HYSPLIT model in order to determine if any masking of Hoppel minima by anthropogenic or natural aerosols is occurring. If evidence of masking can be shown alongside cloud cycling in the sample area, then it is hypothesized that the Hoppel Minima may still be occurring but we are unable to see it directly.

Air trajectory analysis can also give insight into the aerosol itself. Vertical motions can reveal whether the aerosols were lifted high enough to be processed. The trajectories can also yield an estimate of where the aerosol originated and therefore give a reasonable estimate of what type of aerosol it is and its characteristics.

Utilizing the NARR 32-km database, three different runs of the HY-SPLIT model were used. Each run focused on certain heights: surface, 500m above ground level (AGL), and 1000m AGL. Each run initiated at the ARM SGP central facility, located at 36.605°N, 97.485°W. Vertical motion of the air was calculated from the model vertical velocity. The first run consisted of 24-hour long back trajectories run every 3 hours for each of the eleven days. These short runs allow analysis of what has most recently affected the air and what may be causing changes to the spectra on a relatively shorter timescale. The second run focused on the origin of the air by using 168-hour long back trajectories run every 6 hours, allowing analysis of both the origin of air (e.g. maritime or continental) and what environments the air had been exposed to over the previous week (e.g. did it pass over a large urban area or stay over farmland). Finally, a third set of runs was used to primarily see if precipitation occurred in the back trajectory by observing rain rates along the back trajectory. Hoppel et al. (*1986*) noted that the minimum observed was after non-precipitation cloud cycles; therefore comparisons of spectra can be made between those with precipitation in the back trajectory versus those without precipitation.

Satellite and Surface Analysis Methods

Satellite imagery from the University Corporation for Atmospheric Research (UCAR) Mesoscale and Microscale Meteorology Laboratory database is an extremely helpful tool to see the presence, amount, spatial distribution, and type of clouds in the area of the SGP site. Images from the database will be closely studied and compared with pyranometer (solar radiation) data, air trajectory analysis, and the estimated CCN modal

ratings in order to get a broad idea of the cloud cycling occurring or not occurring during the sampling periods.

The various parameters that will be studied in the satellite images are necessary to understand the cloud processing system as a whole as well as the fact that some of these features may not have been as thoroughly examined in previous studies. For example, cloud type has often been limited to marine stratocumulus, stratus, and cumuli (e.g. *Hudson 1982; Hoppel 1996; Hudson and Noble, 2013, 2014 etc.*) which occur frequently over the ocean, where the majority of Hoppel Minima studies have taken place.

The ARM network has a large number of useful tools in order to know the conditions of the sampling periods. Images and movies of sky cover can also be combined with satellite data in order to see the clouds that were occurring before, during, and after CCN samples were made. Numerous other parameters are available from the website, such as vertical motion, liquid water content, soundings, and radar reflectivity, can be used for specific cases as needed in order to complete the picture of what the atmospheric conditions were like on the day in question.

Surface observation data is also necessary for determining the cloudiness of the sampling period. Utilizing the MMM UCAR database once again, surface observations from nearby stations in the MesoWest network – primarily Ponca City, Woodward, and Oklahoma City, OK – can give insight into cloudiness, precipitation reaching the surface, wind speed and direction, and current surface temperature and dewpoint temperature.

Combining the large amount of data from the ARM network with satellite and MMM UCAR surface data will yield a complete spatial and temporal picture of the SGP

site. Combinations of various data may change depending on the case and unique features seen in the data such as strong inversions in the boundary layer, precipitation, or cloudy days with no observed bimodality and vice versa. This will all be used in order to classify each observation day into one of four cases: 1) Sunny Days, 2) Overcast mornings with cloudy afternoons 3) Cloudy Days and 4) Overcast days. Each case type will be examined more closely in the next section.

Case Overviews

Time of Day Cases

All of the 268 observations over the eleven sample days were separated into 7 time periods in order to observe connections between aerosol parameters and time of day. These seven periods consisted of two primary periods, Day (0600-2100) and Night (2100-0600), and five secondary periods, Late Night (0000-0500), Morning (0500-1000), Midday (1000-1500), Afternoon (1500-2000), and Evening (2000-2400). The number of times within each date as well as the number of bimodal cases observed per time period per day can be seen in Table 3.The midpoint of each measurement time period was used to sort the measurements into their periods. Within these periods the relationships between modal ratings, time of day, total N_{CCN}, as well as the distance between bimodal peaks (S_u-S_p) is shown.

The distance between the peaks is characteristic of the shape of the spectra. Larger S_u-S_p indicates greater separation between the modes. On average, S_u-S_p increases with modal rating (Figure 5). This is also the case for each of the time periods except for

Midday, during which S_u-S_p decreased with increasing modal rating, however it is only weakly correlated and not statistically significant with R = -0.32 and SL = 93.7% (Figure 6). S_u-S_p may not be a consistent indicator of the characteristics of the CCN spectra. S_P is assumed to move relative to the location of the original monomodal peak, which can show the amount of processing that has occurred. However, S_U can also move due to Brownian capture of the unprocessed CCN, ultimately leading to a lower S_U. N_u-N_p, on the other hand, seems to be a better indicator of the amount of processing that has occurred. If N_u-N_p is negative, the amount of processed CCN is greater than the amount of unprocessed and therefore more cloud processing is indicated. N_u-N_p for the peak N_{CCN} (the maximum individual concentration of each mode; Figure 7a) and for the integrated N_{CCN} over the entire mode (Figure 7b) against modal ratings both show an increase in the amount of processed CCN with larger modal ratings.

The increasing amount of processed CCN is also shown by Figure 8. When averaged over each of the five time periods (Late Night, Morning, etc.), N_{CCN} reaches a minimum at Midday (Figure 8a) while the modal rating reaches a maximum (Figure 8b). Higher modal ratings should correspond to more unprocessed air (*Hudson et al. 2015*) and therefore higher N_{CCN}; however, this does not seem to be the case (Figures 9 and 10). N_u-N_p is also at its most negative point (Figure 9a) at this same time, suggesting that the processed mode is indeed larger than the unprocessed mode. S_u-S_p shows that the modes are well separated (Figure 9b).This may be due to pollution within the apparent processed mode, leading to a nearly monomodal spectra located at lower S_c (S_c < 0.3%) than idealistic monomodal spectra (S_c > 0.3 %), which are generally assumed to be unprocessed. The influence of pollution may also explain why this feature is much more

prominent during daytime hours, when emissions from human activities are usually higher. Exceptions would include nighttime hours with strong inversions, which would keep pollution trapped near the surface; this may explain why N_u-N_p for Late Night is more negative than Evening (Figure 9a), as inversions are more common in the early morning hours.

Case Type One: Sunny Days

Case type one was defined as days that were clear with less than 10% cloud cover during the majority of the day. This case type, by definition of being nearly cloud free, should also be precipitation free. Of the eleven days of data, only May 11 fit into this case type. The average modal rating, measurement durations, and U/P rating can be seen in Table 4. Figure 10 shows the average modal rating with time. Measurements on this day occurred during the afternoon and evening. The cloud cover was minimal during the entire day, never reaching above 10%.

Back trajectories were run for 24-hours and 168-hours (7 days) at 0m, 500m, and 1000m above ground level (AGL). The air at the surface originated from the Northern Plains 24 hours before each run. From 09z May 11 to 06z May 12, the 24-hour runs showed the surface air being lifted to 500-1500m AGL over Nebraska and Kansas before descending in south central Kansas. This significant lift may suggest interactions between the sampled air and clouds, especially from 15z May 11 to 5z May 12 which coincides with the measurement periods. The air was at a maximum of 1500m AGL at approximately 22z May 10 near southwestern South Dakota and satellite imagery confirms that clouds were present at that time and location, shown in Figure 11. Locally,

there was a general sinking motion as seen by the ARM derived ω (a parameter that describes vertical motion and can be estimated from the vertical wind, W, by using the relationship $\omega \propto -\rho g W$ where ρ is the density of air in kg m^{-3} and g is the gravity constant of 9.81 m s^{-1}) function and the vertical velocity determined from the wind profiler located at the ARM SGP central facility in Lamont, Oklahoma (Figure 12). This reinforces the low modal ratings seen from just before 1900 CDT to 2100 CDT. The apparent spike in modal ratings seen in Figure 10 at 2100-2300 CDT may be due to the upward motion seen in Figure 12 at the same time. The cloud-processed air was not being allowed to descend to the surface and this suggests that surface concentrations may have influenced the modal ratings. This hypothesis is supported by the U/P rating, which shows the spectra shifting from "III – unprocessed" to "I – mono unprocessed" (not shown). The total concentration of the CCN also increases between 2200CDT and 2300CDT, suggesting an influx of unprocessed aerosols. However, since this is only one measurement period, the relationship between vertical motion and the U/P rating system needs to be examined further on other days.

Case Type Two: Cloudy Mornings

Case type two was the most common case observed during the eleven days of this study. This type was defined by an overcast or cloudy morning that transitioned to partly cloudy conditions by mid-afternoon. May 13, 14, 23, 24, and 25 were all classified as case type two. Of these five days, precipitation occurred on three days (14, 23, and 24). The modal ratings, duration of measurement periods, and U/P rating are shown in Table 4. The modal ratings of all five days in this case type can be seen in Figure 13. A diurnal

trend can be seen in the modal ratings, with monomodal spectra peaking during daytime with predominately bimodal spectra at night. Statistical analysis confirms that this relationship is correlated (R = 0.58 SL = 100.00%).

The 24-hour back trajectories do not reveal any vertical motion in the air arriving at the surface, unlike type one, however, the vertical velocity does show a sinking motion over the local area during the afternoon of four of the five cases. On precipitation days, the sinking was much stronger during the precipitation events. On May 23 and 24, significant rain moved over the measurement site and both events registered relatively fast (greater than 4 ms^{-1}) sinking. CCN measurements only occurred during two of the three precipitation events and both were associated with a U/P rating of "II – unprocessed bimodal" after the precipitation event. Figure 14 shows the difference between the three precipitation days and the two non-precipitation days. On days with no precipitation, the diurnal cycle is prominent. However, on the precipitation days, the spectra remained consistently bimodal and with CCN number concentrations an order of magnitude higher than the non-precipitation days. This may be due to the stronger sinking on precipitation days, allowing higher concentrations of CCN that exist above the surface to be transported downward.

While looking at the combined days as a whole, N_{CCN} on the precipitation days was higher (Figure 15b) and had a lower mean U/P rating (Table 4), suggesting that air with a larger processed mode was being sampled. By this reasoning, the non-precipitation days may be more processed. The decreasing trend seen in Figure 15a is present in both individual days, however the decrease is much larger on May 13 than May 15 for part of

the day. The steep decrease on May 13 is also seen in the U/P rating, transitioning from "VI – monomodal processed" to "IV – processed" by approximately 1700 CDT when a break in the cloud cover was recorded by a nearby MesoWest station. The back trajectory for May 13 suggests that the air passed over the Oklahoma City metro area within six hours of the measurements. The air measured on May 25, however, did not pass over any large urban areas but instead remained over rural areas. Anthropogenic aerosols may have then played a role in the much larger N_{CCN} values on May 13 and may also explain the presence of the so-called "processed monomodal" spectra. Both days had a sinking motion seen in the vertical velocity during the periods of rapid decrease of N_{CCN}, giving evidence that cloud processed air could be reaching the surface. The U/P ratings also shift at this time to bimodal ("II – bimodal unprocessed" on May 13 and "IV – processed" on May 25).

The precipitation days also showed differences in N_{CCN} depending on the origin of air shown in the back trajectory. May 14, like May 13, passed over urban areas before reaching the measurement site. During the early portion of that day, the surface air traversed Oklahoma City and as the day progressed the trajectory briefly passed near Tulsa. Similar to May 13, when the air had directly passed over an urban area, N_{CCN} was relatively larger than N_{CCN} at times where it had only been exposed to rural areas. However, since the trajectory was shifting during the day, N_{CCN} decreased to values typical of rural back trajectories for this study. The U/P rating does not show evidence of a strong urban influence like that of May 13 and instead remains between "IV – processed" and "II – bimodal unprocessed". May 23 and 24 both have rural back trajectories and similar U/P ratings, remaining within the boundaries described for May

13. Spikes in the N_{CCN} were near the same time precipitation was occurring for both May 13 and May 23. CCN data during precipitation was not available on May 24. Precipitation may also have an impact on N_{CCN} even after it has passed the measurement area; all three precipitation days saw decreases in N_{CCN} after precipitation ceased. Transport of cloud processed air to the surface is again supported by a sinking motion in the vertical velocity (Figure 16).

Case Type Three: Cloudy Days

Case type three encompasses days that were "partly cloudy." Clouds were present during the majority of the day but did not reach overcast conditions. Two days, May 22 and May 26, fit into this case type. Neither day had precipitation. The statistics of the case type, modal ratings, duration of measurement periods, and U/P rating are shown in Table 4.

Twenty-four hour back trajectories have the surface air originating in northeastern Kansas, near St. Joseph and Kansas City. On May 22 the air was not lifted above the surface before arriving at the measurement site but remained on a primarily rural trajectory during the entire time period. May 26 did have minor lifting occurring at 12z May 25 to 00z May 26 near the Kansas-Missouri border south of Kansas City. Visible satellite from this time period confirms cloud presence, indicating that cloud processing may have occurred on May 26.

On both days, clouds were locally present. Vertical velocity obtained from wind profiler data shows intermittent sinking and rising motions after 1000 CDT on each day (Figure 17). Above 1 km the sinking and rising motion oscillations are much more

extreme, suggesting the presence of clouds. LIDAR data obtained from ARM shows what appear to be small clouds between 1 and 2 km altitude on both days, both beginning at approximately 1000 CDT. Cloud processing of CCN and bimodality at the surface is further confirmed by the U/P ratings for each day, with mean U/P ratings of 3.18 and 3.41 for May 22 and May 26 respectively (Table 6). After 1000 CDT, the U/P rating switches from an unprocessed dominate mode (lower U/P rating) to a processed dominate mode (higher U/P rating) (Figure 18). Bimodality of the CCN spectra is also confirmed, with ratings becoming bimodal after being exposed to the cloudy conditions and intermittent sinking.

From Figure 19 two monomodal peaks appear to occur in the modal ratings, with one at noon and the other near midnight. These peaks occurred only on May 22 as the modal ratings on May 26 were all "1." On May 22 the conditions were clear until 1100 CDT when clouds began to form in the vicinity whereas on May 26 fog was present in the morning. A sinking motion appears in the vertical velocity just before 1500 CDT on May 22, which is when the mode changes from monomodal to bimodal, suggesting cloud processed air may be reaching the surface, however, there are no measurements during this period to confirm this. This hypothesis is further supported by the increase in modal rating at the same time the vertical velocity approaches zero (Figure 17a). Air trajectory analysis also presents two differences: May 26 had recently (less than twenty-four hours before measurements) descended from 500-1000m AGL over west-central Missouri while air on May 22 remained near the ground with much closer origins. The shift from primarily unprocessed air to processed air can also be seen in the U/P rating and N_{CCN} time plots (Figure 20). The U/P ratings decrease from "VI – monomodal processed" to

"IV – processed" by 1600 CDT on May 22 (Figure 20b), possibly suggesting cloud processed air as in previous days; however, N_{CCN} is increasing during this period. This increase may be due to pollution accompanying any cloud processed arriving air. Back trajectories reveal that the air had passed over Kansas City within 72 hours of the measurements, which may account for the processed spectra with increasing N_{CCN} during the majority of the day. By 2000 CDT, the arriving air has not passed near the surface over any major cities and N_{CCN} has decreased accordingly. Figure 21 describes N_{CCN} for both the unprocessed and processed components of the spectra. When comparing May 22 (Figure 21a) to May 26 (Figure 21b), a bimodal day with consistent modal rating of 1, it can be seen by 2000 CDT on May 22 the unprocessed and processed total N_{CCN} approach each other similar to May 26.

Case Type Four: Overcast Days

Overcast days were classified as case type four. May 15, 16, and 17 were overcast the majority of the day, with cloud cover 90% or greater. Precipitation occurred on May 15 and 16 with a convective thunderstorm passing over the ARM central facility on May 16. The statistics of the case type, modal ratings, measurement durations, and U/P rating are presented in Table 4.

On both of the precipitation days, an increase in the modal rating was seen after the precipitation ceased. Both days also had lower mean N_{CCN} than days without strong precipitation (Table 5). An interesting difference, though, is that N_{CCN} on May 16 decreased after precipitation and the total processed N_{CCN} decreased while the unprocessed decreased only minimally (Figure 22). This may be due to the fact that the

precipitation was from a strong thunderstorm on May 16, whereas the precipitation on May 15 was not as significant. At the surface, May 15 and 16 had oscillations of significant rising and sinking motions while May 17 remained near neutral, with some sinking occurring. The 24-hour back trajectories do not initially reveal much of interest other than that the air at the surface had remained on a rural path the majority of the time.

Figure 23 shows a diurnal trend in the modal ratings once again, with a peak occurring later than what was common in case type two. However, as May 16 only had measurements during the morning and the measurements of May 17 were during the late afternoon and evening, there is only May 15 to truly observe a diurnal trend. The modes did increase in the first five hours of the day and decreased after sunset, but with an observed maximum just before sunset (Figure 24). This may be due more to the precipitation discussed earlier than to a true diurnal oscillation of the modal rating. Further twenty-four hour measurements on overcast days, with both precipitation and no precipitation, would need to be conducted in order to determine the existence of an oscillation in this case type.

The U/P rating also had significant differences between precipitation days and non-precipitation days. May 15 and 16 had an average U/P rating of “II – unprocessed bimodal” while May 17 had an average between “V – processed bimodal” and “VI – processed monomodal” (Table 6). N_{CCN} was also significantly larger on May 17 and, as stated earlier, had variable weak vertical velocity. Similar to May 22 in case type three, the large N_{CCN} and the large U/P rating may be due to anthropogenic influences. Back trajectories a week before this date are also similar to those of May 22, with the surface

air passing over Kansas City less than 48 hours before the measurements. This may imply that the origin of air has a stronger influence on the CCN observed at the surface than downward transport, for either processed or unprocessed.

Results

Is the Hoppel Minima occurring?

As stated in the previous section, it has been shown that the Hoppel Minima is being observed at the surface in Oklahoma due to cloud processing and there is evidence of transport of cloud processed air to the surface. Table 5 shows the average location of the Hoppel Minimum for all eleven days. Days with stronger convection and therefore stronger in-cloud updrafts, such as case types two and four, had Hoppel minima at higher S_H than days with weaker updrafts, such as case type three (Table 4). The lowest mean S_H, 0.24%, on May 11 was classified as case type one, with clear and sunny conditions. The largest mean S_H, 1.03%, occurred on May 17 which was discussed in Section Case Type Four: Overcast as having features more influenced by anthropogenic pollution than cloud processed air. The air had also passed through significant precipitation in the back trajectory, probably due to the convective features of the storms.

The overall average location of Hoppel Minima (S_H) is 0.68% which is higher than previous studies. This is expected due to the different types of clouds occurring over land than over water. *Hudson et al*. (2015) showed S_H near 0.3% S_C with higher values occurring in ICE-T (S_H = 0.44%) than MASE (S_H = 0.15%), due to the difference in updraft velocity between cumulus and stratus clouds, respectively. *Hoppel et al.* (1996)

also estimated similarly low values of the in-cloud S_{eff} in the tropical marine boundary layer. Due to this reasoning, the average S_H in Oklahoma is higher than S_H observed over the ocean.

Is cloud processing occurring?

The presence of Hoppel Minima can be further confirmed by showing that cloud processing is occurring. In order for cloud processing to occur, two conditions must be fulfilled: clouds must be present in the area or in the immediate back trajectory (ideally less than 72-hours along the trajectory) and there must be transport of air from cloud to surface. These conditions should be present on days with bimodal spectra. Bimodal spectra were observed on each of the eleven case days (Table 6) and a modal rating of 4 or lower was recorded at least once per case day.

For ten of the eleven case days, clouds were present near the ARM SGP central facility during the majority of the day; these days were discussed in case types two, three, and four. Transport from cloud to surface was indicated by the vertical velocity for each of the case days, even for very miniscule motions such as on May 13 (Figure 25b). The sinking motion can account for cloud-to-ground transport on nine of the eleven case days, excluding May 11 (case type one; no clouds present) and May 13 (where minimal downward transport was observed). On both of these days, bimodal spectra were still observed and in order to be attributed to cloud processing, further explanation is needed.

May 11, as discussed in Section Case Type one: Sunny Days, had no clouds the entire day and measurement periods. The lack of clouds nearby would seem to make the sinking motions seen in the vertical velocity irrelevant, however the back trajectories and

satellite imagery (Figure 11) do reveal that the air had not only passed through cloudy regions but had also been transported from cloud level to surface level before arriving at the measurement site. This movement of cloud-processed air is accompanied by low modal ratings until the sinking motion switches to rising motion at approximately 2100 CDT (Figure 12). The U/P ratings change from bimodal distributions to "I – monomodal unprocessed" near the same time period. The connections in the modal ratings, U/P ratings, vertical motion, and back trajectories support that cloud processing was indeed causing the bimodality in the CCN spectra.

May 13, on the other hand, did have clouds present and was classified as Case Type Two: Cloudy Mornings. Clouds were indeed present in the area as seen in the increased signal near the surface from the LIDAR data (Figure 26), however, transport to the surface according to velocity in the local area seemed negligible (Figure 25b). Figure 27 does show that the modal ratings agree with a lack of transport of cloud processed air until 1900 CDT when the ratings decrease to those corresponding with bimodal spectra. At this time the cloud cover had begun to break (Figure 26) and the small – yet still present – sinking motion appears in the vertical velocity, especially near 0.5 km above the surface. While it is a much less noticeable sinking motion than the other days, it is accompanied by a sharp decrease in N_{CCN} (Figure 28a) and a decrease from a U/P rating of "VI – processed monomodal" to "IV – processed" (Figure 28b). There is also a shift in the back trajectory from a path leading over the central I-35 corridor (causing the contradictory "monomodal processed" spectra) to slightly west of the main urban corridor (more rural), which may have also led to the reduction of N_{CCN} and the U/P rating (Figure 29).

If cloud processing is occurring it can also be seen in the κ values assigned to the CCN spectra. Processing can cause κ to shift and perhaps differ between unprocessed and processed mode. The processed κ should be greater than the unprocessed κ. A difference in the best-fit kappa can be seen in at least one measurement in ten of the eleven case days. The mean value of K_u-K_p is +0.26, revealing that the processed κ is smaller than the unprocessed κ and suggests anthropogenic sources may have influenced the processed air. While this does seem contrary to the hypothesis of cloud processing, it only occurred for 58 of the 268 cases.

Overall it can be concluded that cloud processing is indeed occurring as there are consistently clouds present either in the immediate area or back trajectory. Transport from cloud level to surface can be seen for the majority of the bimodal spectra. Therefore, it is concluded that the minimum seen between the bimodal CCN spectra is indeed caused by cloud processing and thus the Hoppel Minima is observed.

What conditions lead to the formation of the Hoppel Minima?

Whether or not the Hoppel Minima could be observed at the surface depended on two main factors – did the air recently pass over a large urban area and is there enough downward vertical velocity (sinking) to transport the cloud processed air? Clouds in the immediate area of the measurement site were not necessary as seen on May 11. If ample clouds were present in the back trajectory within the previous 72 hours, then the clear conditions often associated with widespread sinking motions (due to an atmospheric ridge or surface high pressure for example) may assist in transporting cloud processed air to the surface.

In Case type four, observations made after significant precipitation did appear to mask any bimodal features seen in the spectra and also led to more unprocessed ratings in the U/P system. This is consistent with *Hoppel et al*. (*1986*), which specified that the air needed to pass through non-precipitating cloud cycles in order to create the minimum. Case type two is not as easily distinguished; the precipitation days had a larger N_{CCN} (Figure 15b) and lower U/P rating (Table 4), which by the reasoning in the previous section suggests unprocessed air. These were also consistently bimodal, with modal ratings remaining at or below 4 (Figure 14b). This difference may be due to the fact that the precipitation on case type two days was, on average, weaker than the precipitation observed on case type four days.

In two of the four case types, a true diurnal oscillation in the modal rating could be observed (such as those seen in Figure 14a and Figure 22). Days with precipitation did not reach as high a middy maximum as non-precipitation days, which remained bimodal for the majority of the day. The peak on all overcast days occurred later in the day (Figure 22) than peaks on days with only overcast mornings (Figure 13). However, of the five days that truly fit the diurnal pattern - May 13, 15, 16, 17, and 25 – only May 13 and May 15 had twenty-four hours of continuous measurements. The peaks near midday on these days were attributed to factors that are not always apparent; for May 13 it was hypothesized to be due to anthropogenic influences in the back trajectory as well as cloud cover and for May 15 it was due to precipitation occurring at the measurement site. Thus, the diurnal cycles observed on five of the eleven case days are due to numerous factors.

Conclusions

Suggestions for future continental Hoppel Minima research

In order to fully understand cloud processing in a continental environment, further studies are required. A larger sample size of different meteorological cases would allow factors like precipitation, convection, and different types of clouds to be more accurately related to the amount of processing that occurred or did not occur. For example, sunny clear days like those of Case type one may not always have processed, bimodal spectra and depend highly on the origin of the air being sampled. Strong precipitation days, like May 16, may show interesting features in the modal ratings after the passage of a strong convective storm. Continuous measurements would also assist in interpreting the role of meteorology and time of day on the modal ratings as well as determining causes of features seen in the modal ratings, such as the diurnal oscillation discussed in previous sections.

Furthermore surface measurements would benefit from aircraft measurements of the same kind. Aerosol related studies, such as *Wang et al*. (2007), suggest that surface observations may not be representative of the entire boundary layer, even on well mixed days. This may also be the case with CCN and further use of the CCN spectrometers would be necessary in order to understand CCN in the boundary layer as a whole.

Differences between bimodal days and monomodal days

Of the 268 measurement periods, 218 had an observable Hoppel Minima. Of these 218, 185 had a modal rating of 4 or less, making bimodal spectra more common than monomodal for the eleven day period. Only two days, May 13 and May 17, had more

monomodal spectra than bimodal. These two dates were discussed as having weak vertical velocity and a stronger anthropogenic influence than the other days. Both monomodal days had relatively larger N_{CCN} and a high U/P rating, likely from urban influences. Furthermore, any that cloud processed air was not being allowed to sink to the surface.

Bimodal days, however, each had at least brief periods of the following criteria: sinking motion in the vertical velocity, clouds in the immediate area or recent back trajectory, and no significant precipitation occurring during measurements. These criteria, obtained from a summation of the previous sections, suggest that the cloud processing and therefore Hoppel Minima are occurring over the Southern Great Plains. When it is not observed, it is likely being masked by anthropogenic pollution and a lack of transport of cloud processed air to the instrument.

Tables

Table 1 - Mean, standard deviation, minimum, maximum and total for modal rating and the measurement period length are given for all eleven days. Measurement length periods are given in decimal time and in standard time.

	Modal Rating	**Measurement Period Length (Hours)**	**Measurement Period Length (Standard Time)**
Mean	3.9552	0.4253	25 minutes, 31 seconds
Standard Deviation	2.3203	0.3919	23 minutes, 31 seconds
Minimum	1	0.0167	1 minute
Maximum	8	2.1167	2 hours, 7 minutes
Total	--	113.9808	113 hours, 58 minutes, 51 seconds
Number of Cases	268	268	268

Table 2 – Percentage variation of the N_{CCN} within the averaged measurement periods for six of the eleven days. Five were excluded due to different operational techniques.

Date	Number of Measurements	Standard Deviation	Mean Percentage Variation	Minimum Variation (%)	Maximum Variation (%)
11	12	7.95	6.46	2.09	24.50
17	12	12.04	8.53	3.73	46.52
22	33	3.98	4.32	2.55	25.52
23	43	1.97	4.24	2.10	12.11
24	11	1.97	5.11	3.09	9.62
25	27	1.00	3.83	2.57	6.82

Table 3 - Number of cases with bimodality for the five time periods for each of the eleven days. The time periods are: Morning (0500-1000 CDT), Midday (1000-1500 CDT), Afternoon (1500-2000 CDT), Evening (2000-2400 CDT), and Late Night (0000-0500 CDT).

Date	Number of Cases	Bimodality Cases	Morning Cases	Midday Cases	Afternoon Cases	Evening Cases	Late Night Cases
11	12	11	-	-	2 / 0	9 / 1	-
13	40	11	-	1 / 20	5 / 9	5 / 0	-
14	31	31	12 / 0	5 / 0	2 / 0	2 / 0	10 / 0
15	27	27	7 / 0	3 / 0	3 / 0	9 / 0	5 / 0
16	20	18	11 / 0	2 / 2	-	-	5 / 0
17	12	3	-	-	1 / 7	2 / 2	-
22	33	31	8 / 0	7 / 2	7 / 0	6 / 0	3 / 0
23	48	43	12 / 0	6 / 5	6 / 0	6 / 0	13 / 0
24	11	11	-	-	3 / 0	3 / 0	5 / 0
25	32	20	2 / 5	0 / 7	7 / 0	2 / 0	9 / 0
26	12	12	3 / 0	-	1 / 0	2 / 0	6 / 0

Table 4 - Comparison of the location of the Hoppel Minimum S_H, modal rating, U/P rating with case type, observation period length, and number of bimodal cases for each case type as a whole and including the two subtypes of case type II.

Case Type	Average Observation Length (min)	Standard Deviation Observation Length (min)	S_H	Bimodal/Total Cases	Average Modal Rating	Average U/P Rating
I	9.50	8.64	0.24	11/12	3.83	2.75
II	22.89	19.53	0.76	116/152	4.21	3.52
III	29.07	26.66	0.59	43/45	2.91	3.24
IV	32.85	28.83	0.68	48/59	4.12	2.71
II - No Precipitation	41.71	13.22	0.31	31/67	6.15	4.60
II - Precipitation	47.12	8.28	0.44	85/85	2.68	2.67

Table 5 - The mean values of the supersaturation (S) and CCN number concentration (N) parameters for unprocessed, processed, and monomodal spectra, for each of the eleven days.

Date	**S_u**	**S_H**	**S_p**	**S_m**	**N_u**	**N_p**	**N_m**
11	0.98	0.24	0.16	1.08	28956	11273	56040
13	0.90	0.70	0.27	0.27	2128	10933	18167
14	0.88	0.73	0.33	--	1131	6802	--
15	0.85	0.71	0.39	--	1262	5099	--
16	1.06	0.59	0.42	0.99	1403	2217	
17	1.30	1.03	0.08	0.06	2594	99580	86552
22	0.94	0.70	0.28	0.21	40725	119729	182604
23	1.06	0.84	0.34	0.15	14032	106849	72377
24	1.02	0.69	0.24	--	15937	51555	--
25	0.94	0.69	0.13	0.11	7758	49516	60548
26	0.44	0.28	0.16	--	15611	18209	--

Table 6 – As Table 4, but for all eleven days as well as the mean of all days together.

Date	**Case Type**	**Average Observation Length (min)**	**Standard Deviation Observation Length (min)**	**S_H**	**Bimodal/Total Cases**	**Average Modal Rating**	**Average U/P Rating**
11	I	9.50	8.64	0.24	11/12	3.83	2.75
13	II	13.87	20.30	0.70	11/40	6.85	4.7
14	II	23.68	19.63	0.73	31/31	2.87	2.39
15	IV	35.48	27.61	0.71	27/27	3.15	2
16	IV	32.85	30.82	0.59	18/20	3.5	2
17	IV	26.92	30.98	1.03	3/12	7.33	5.5
22	III	26.76	20.76	0.70	31/33	3.61	3.18
23	II	24.10	13.62	0.85	43/48	3.15	2.74
24	II	40.64	23.96	0.69	11/11	2.09	3.18
25	II	27.28	27.71	0.69	20/32	5.56	4.44
26	III	37.82	40.96	0.28	12/12	1	3.42
All Days	-	0.43	0.39	0.68	218/268	3.96	3.39

Figures

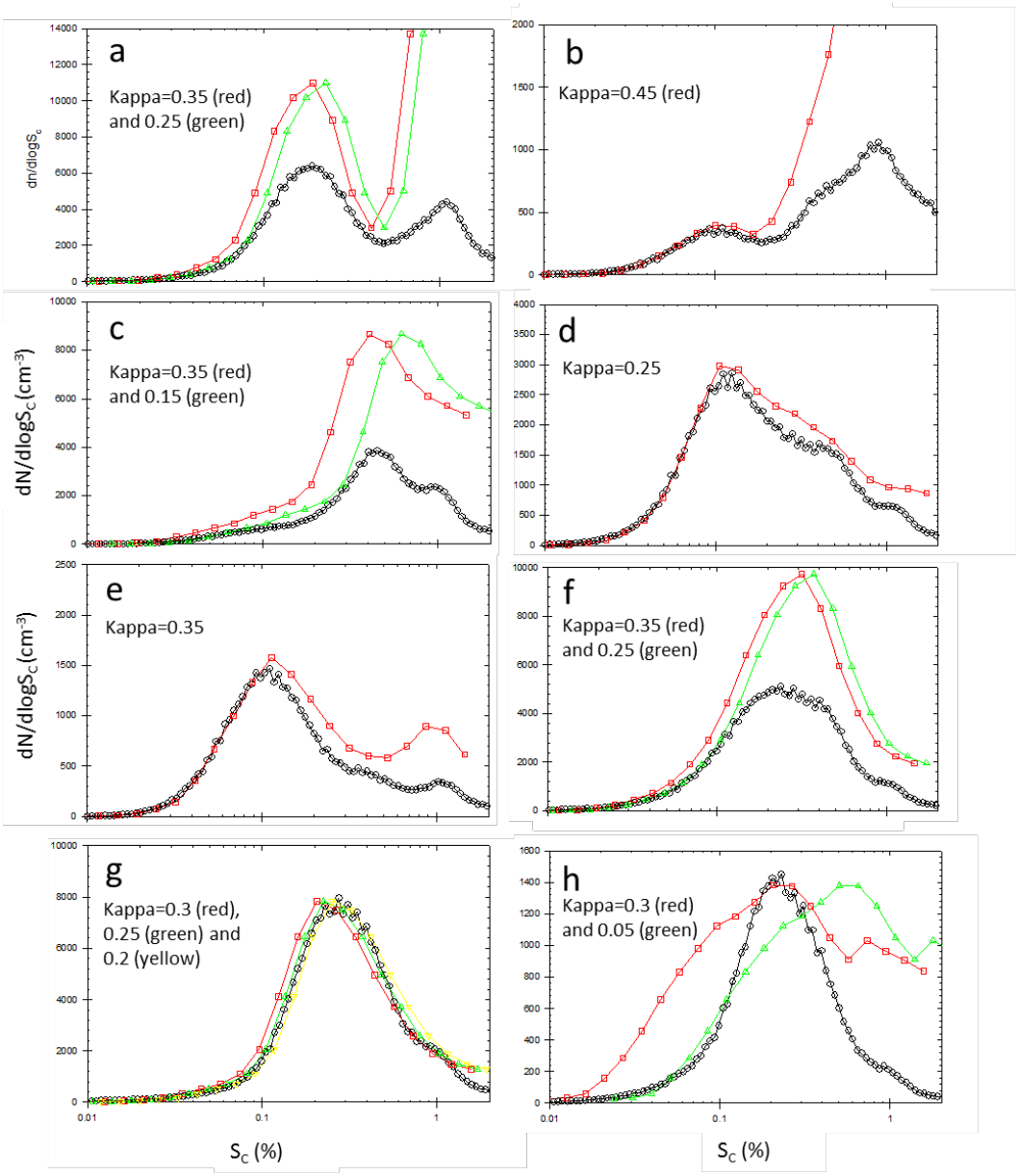

Figure 1 - Differential CCN concentrations ($dN/dlogS_c$) as a function of critical supersaturation (S_c) showing examples of the 1-8 modal rating system (black lines) as well as DMA measurements (red and green lines). (a)rating of 1, May 22 15:25:00-15:39:00; (b)rating of 2, May 11 20:44:30-21:00:00 (c)rating of 3, May 22 00:06:00-00:35:30; (d)rating of 4, May 24 04:01:00-04:30:00; (e)rating of 5, May 25 16:45:00-17:00:00; (f)rating of 6, May 22 11:30:00-11:45:00; (g)rating of 7, May 13 10:15:00-11:04:00; (h)rating of 8, May 13 13:43:00-13:50:00

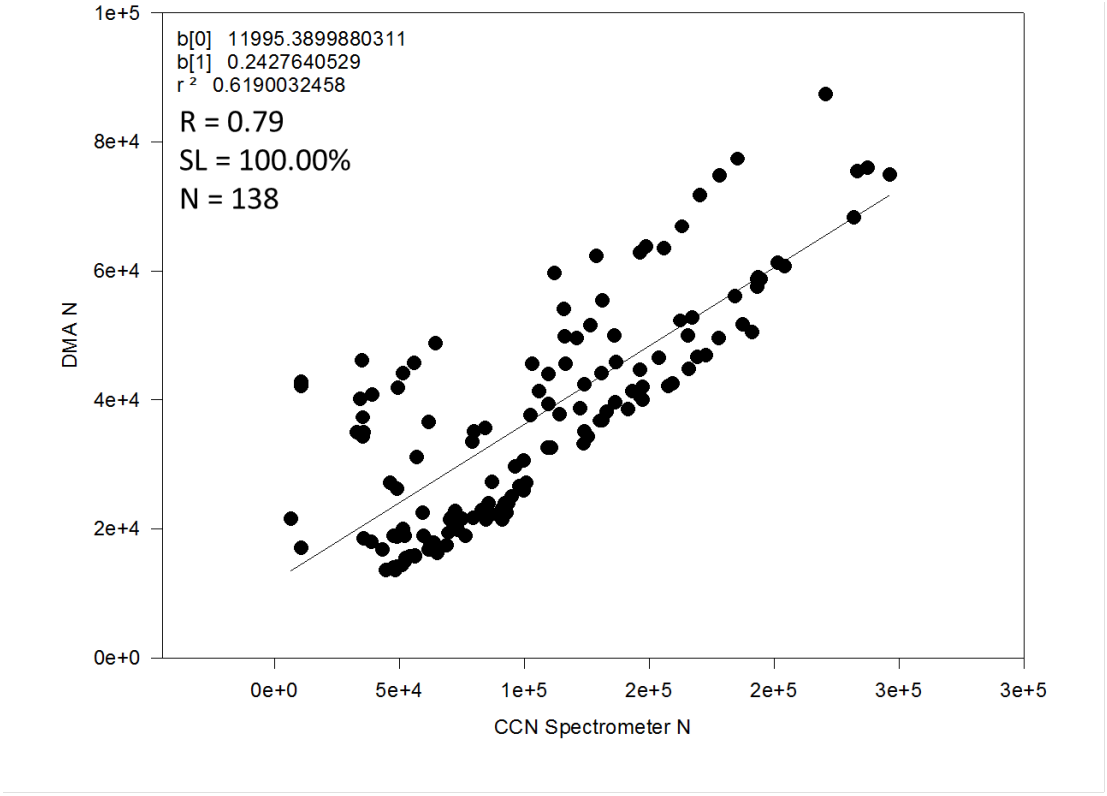

Figure 2 - Relationship between the total integrated number concentration as calculated from DMA observations (y-axis) and CCN spectrometer observations (x-axis). Five days were not included due to adjustments made to the CCN spectrometer.

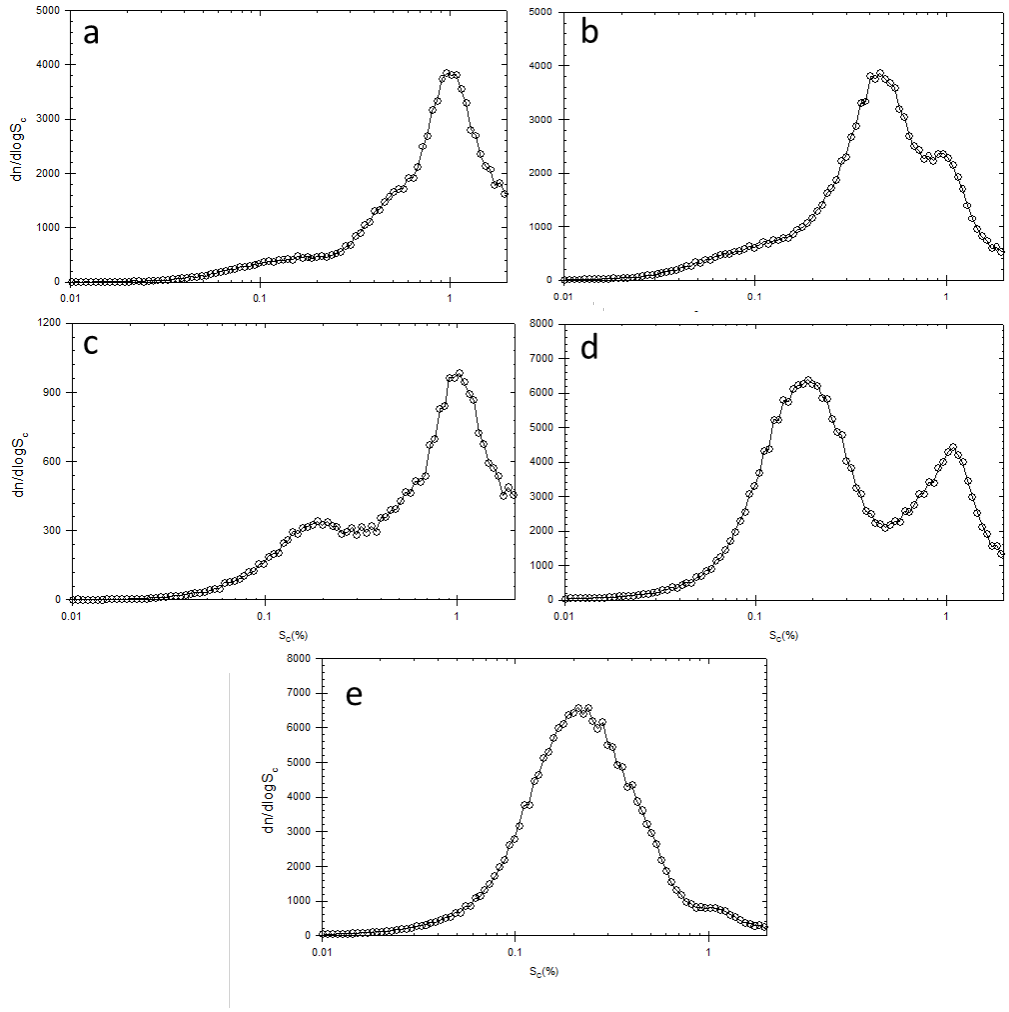

Figure 3 – Examples of the U/P rating system. Note that a rating of "V – bimodal processed" did not occur and is not shown here. a) I – monomodal unprocessed b) II – Unprocessed Bimodal c) III – Unprocessed d) IV – Processed e) VI – monomodal processed

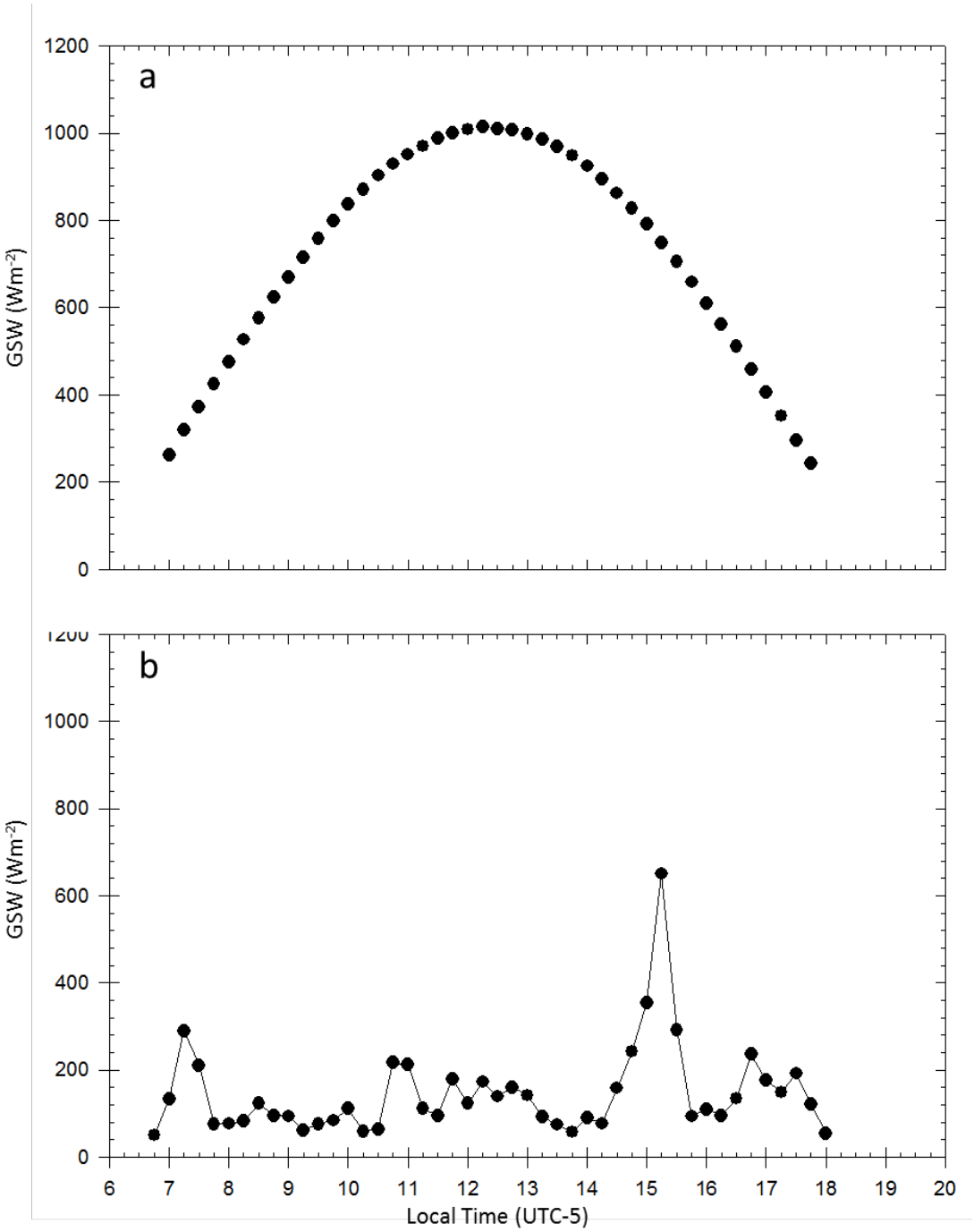

Figure 4 - Plots of global shortwave radiation measurements (GSW) against local time. a)An example of a clear, sunny day. b)An example of a day with clouds present, shown by the interruptions in radiation.

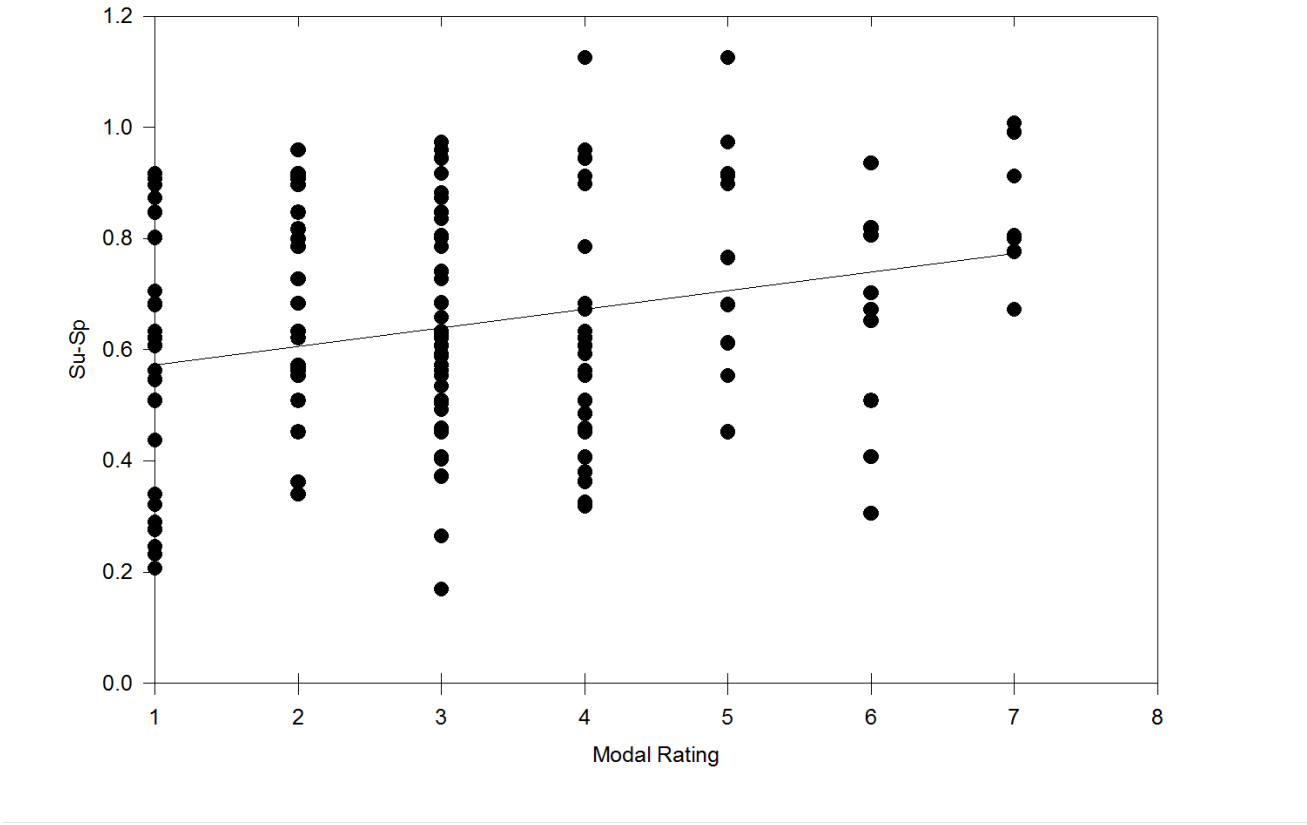

Figure 5 - S_U-S_P with modal ratings for all eleven days.

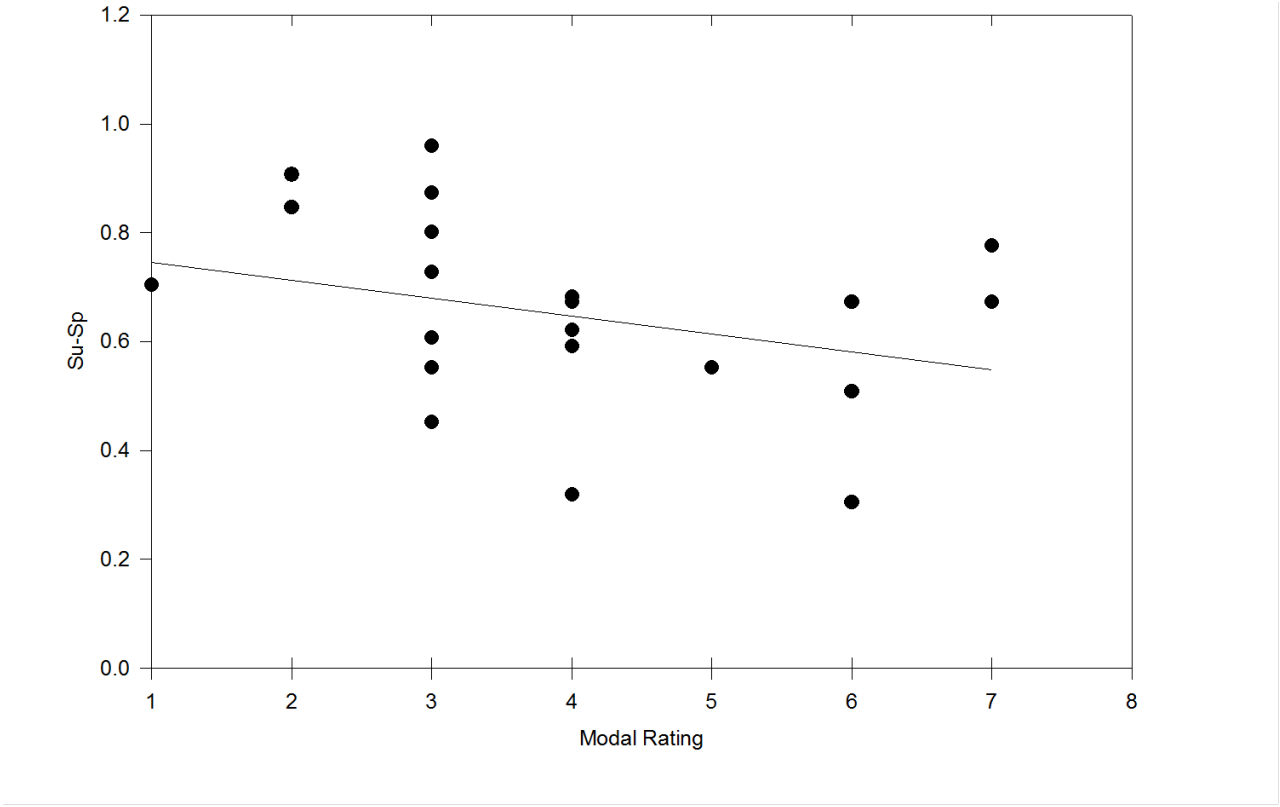

Figure 6 - S_U-S_P with modal ratings for the Midday time period only.

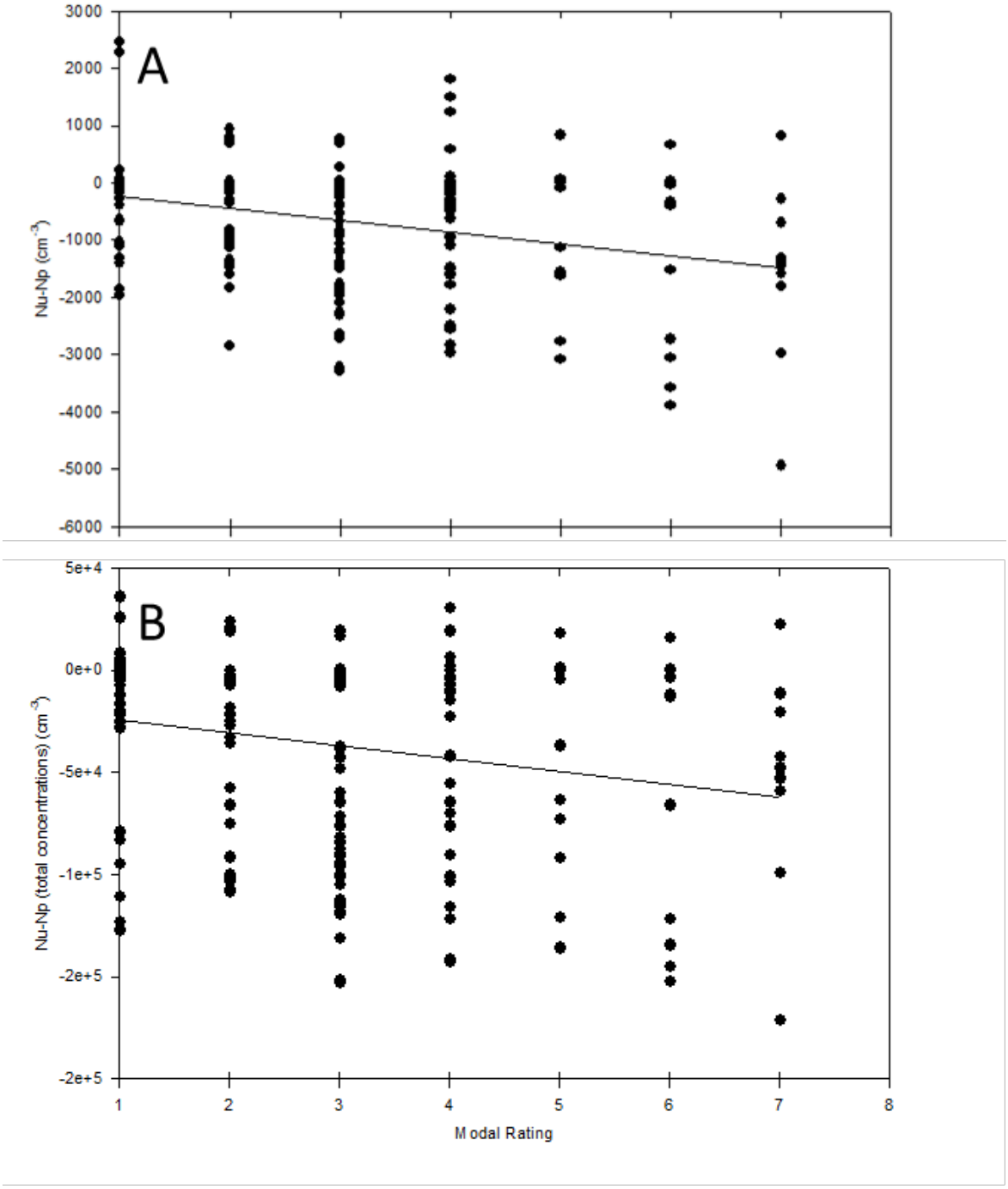

Figure 7 - N_u-N_p against modal ratings for all days. a) Peak N_u-N_p, which is calculated as the difference between N_{CCN} at S_u and S_p. b) Total integrated N_u-N_p

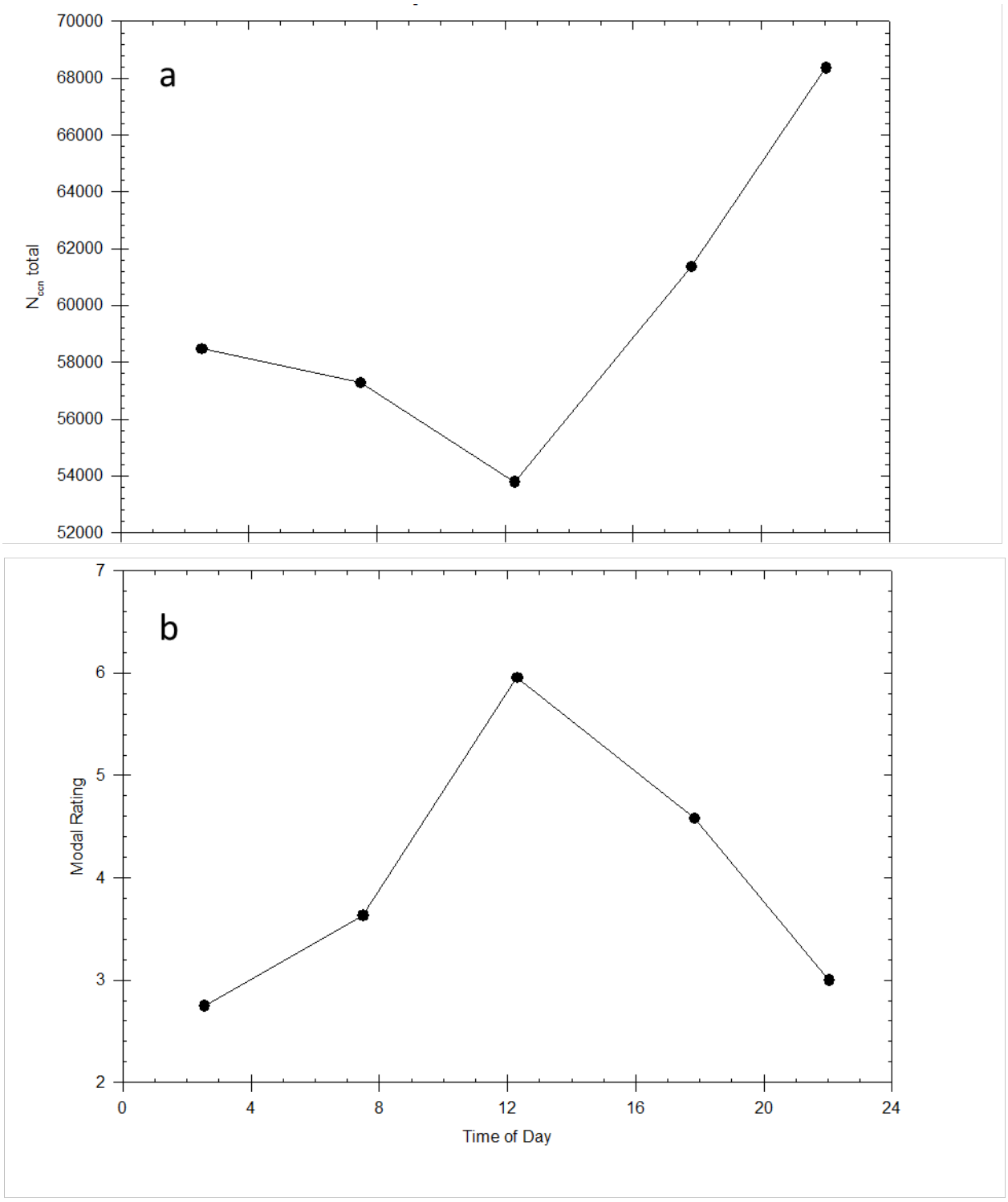

Figure 8 – N_{CCN} (a) and modal ratings (b) averaged over the five time periods for all eleven days.

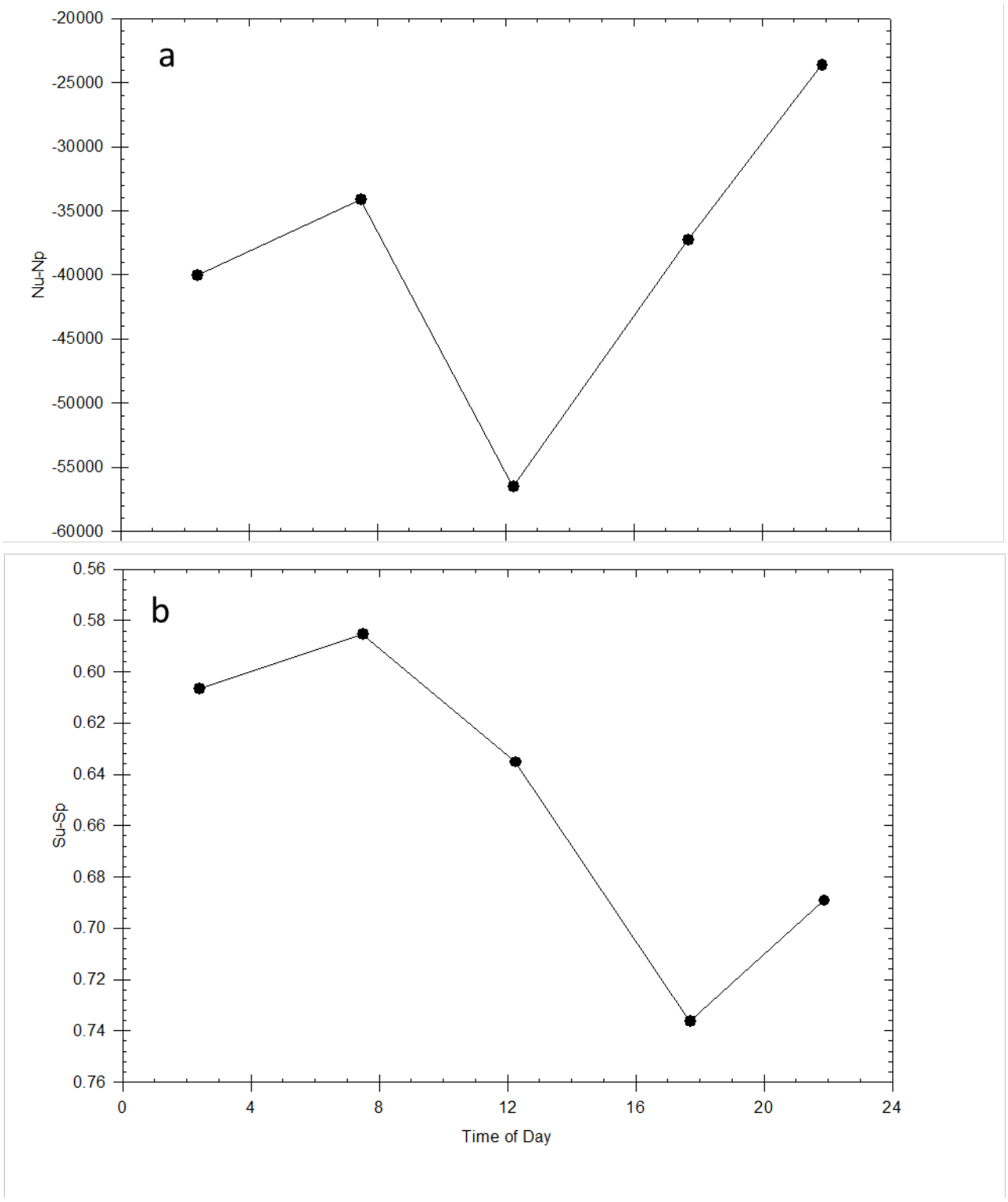

Figure 9 – N_u-N_p (a) and S_u-S_p (b) averaged over the five time periods for all eleven days.

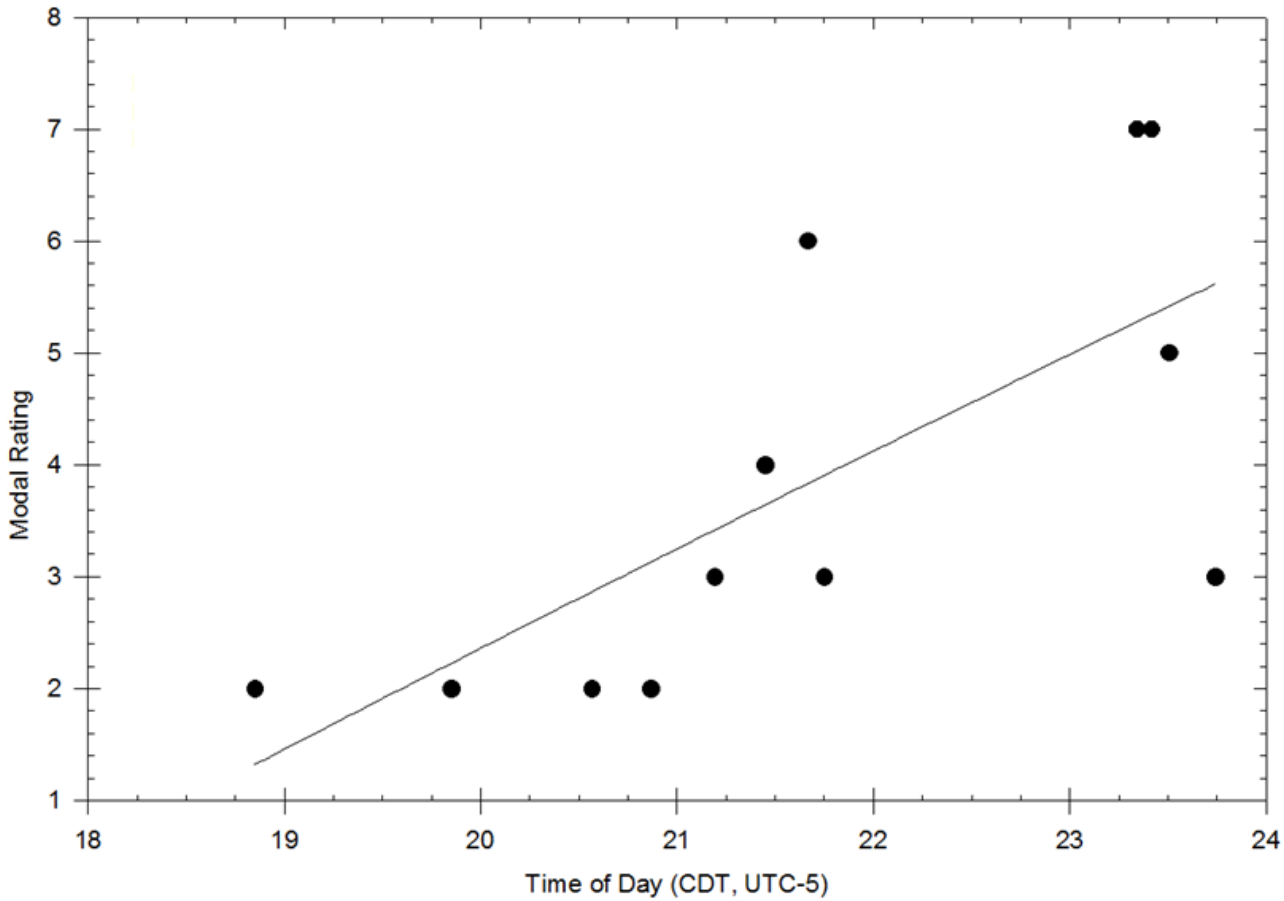

Figure 10 – Modal rating with time for case type one.

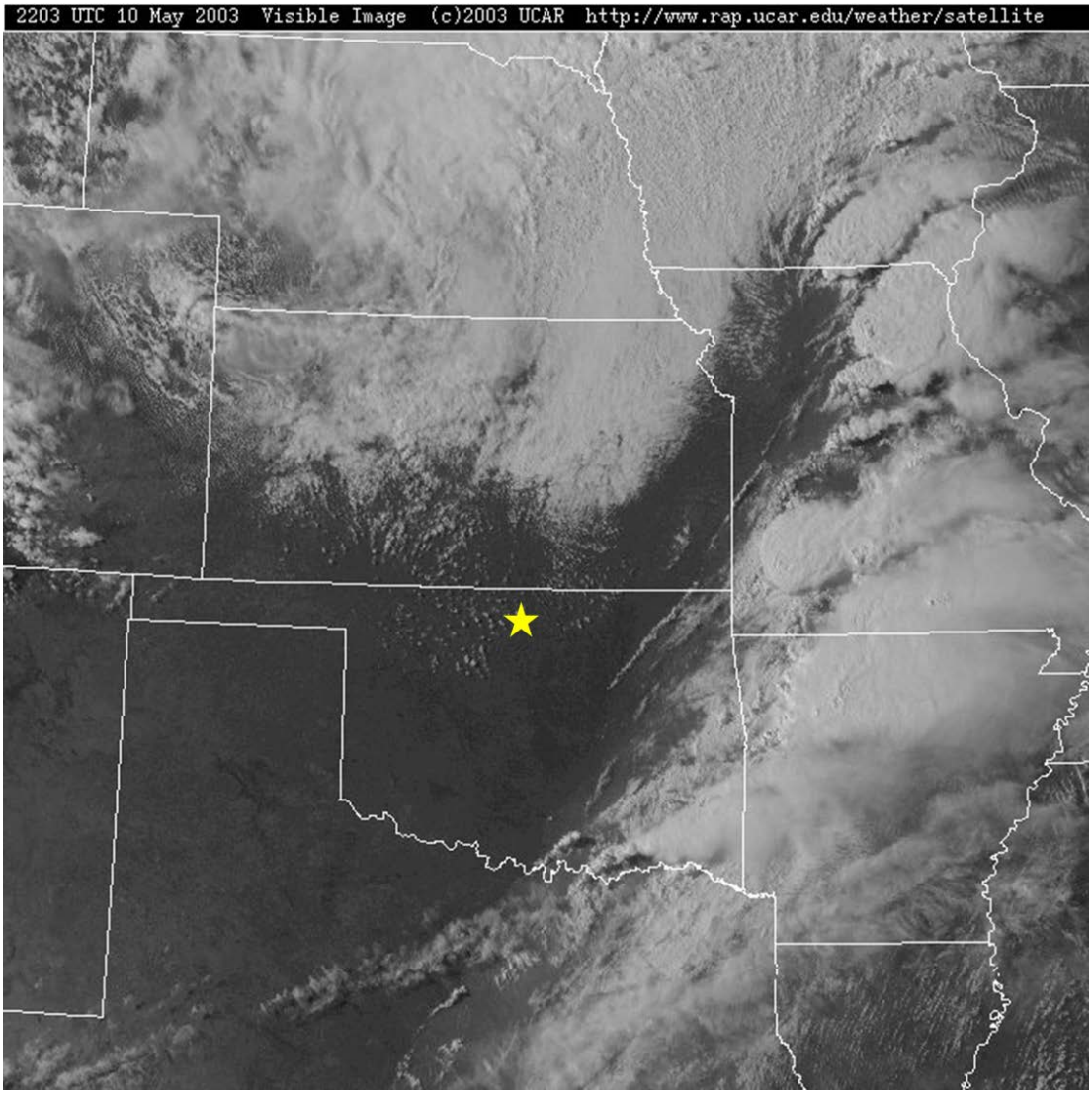

Figure 11 - Satellite imagery from 22z on May 10. Yellow star marks location of the ARM SGP Central Facility, near Lamont, Oklahoma.

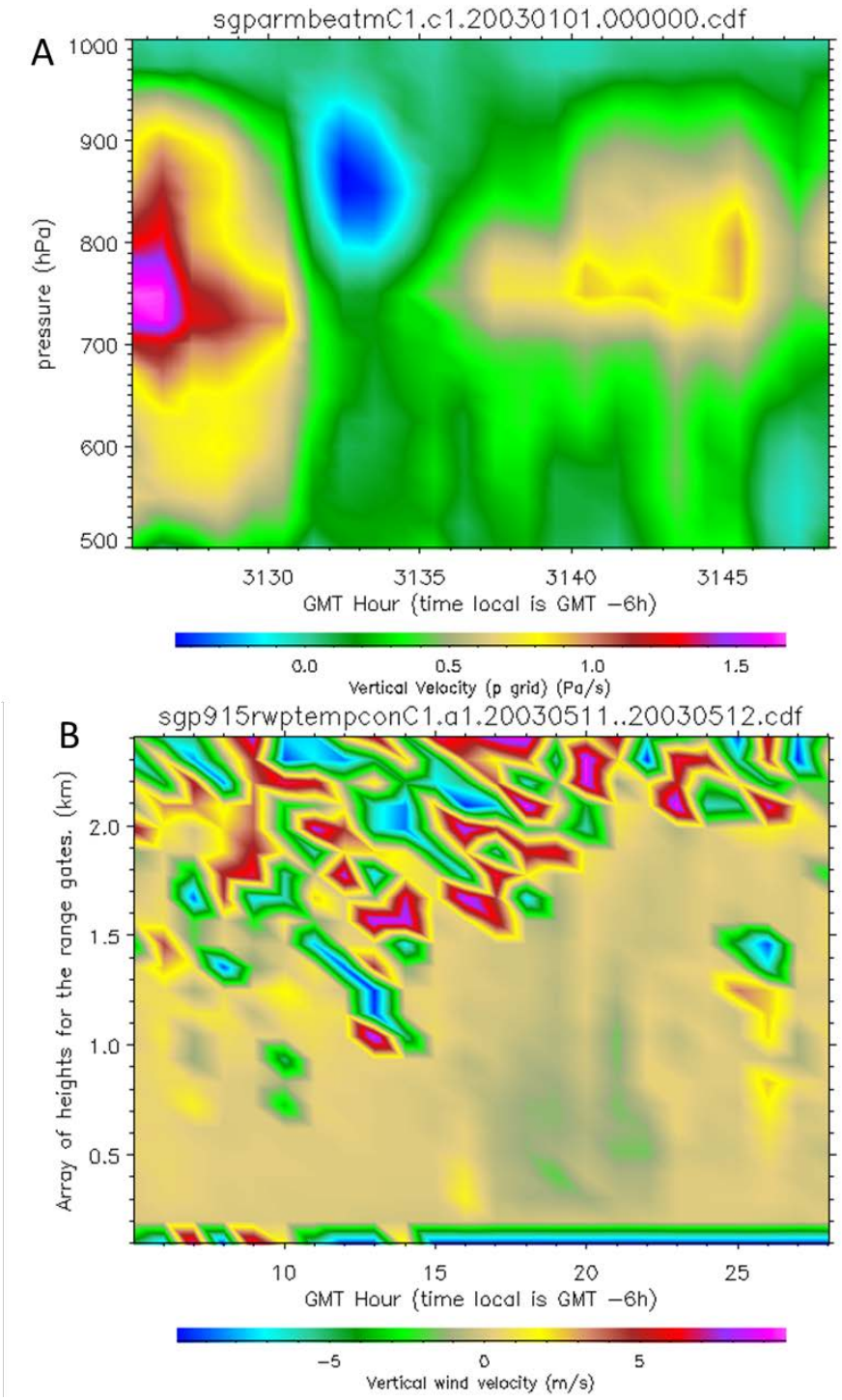

Figure 12 - Vertical motion above the surface on May 11 (05z May 11 to 05z May 12) at the ARM SGP central facility near Lamont, Oklahoma. a) Omega vertical motion in Pa s^{-1} with time from surface to 500hPa. Negative values imply rising motion, positive values imply sinking. b) Wind profiler derived vertical velocity in ms^{-1} with time from surface to 2.5km altitude.

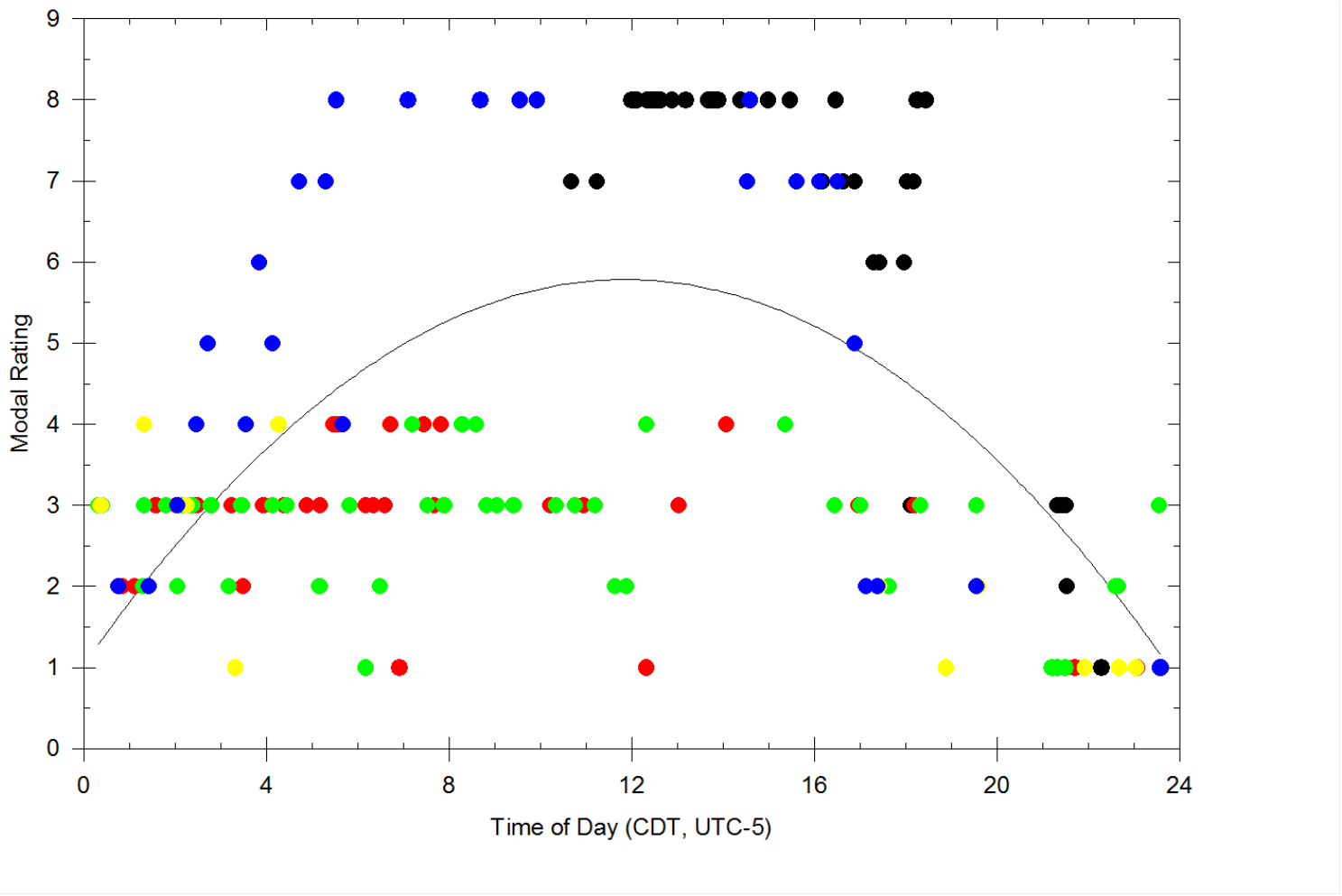

Figure 13 - Modal ratings with time of day for case type two days. Black circles are May 13, red are May 14, green are May 23, yellow are May 24, and blue are May 25.

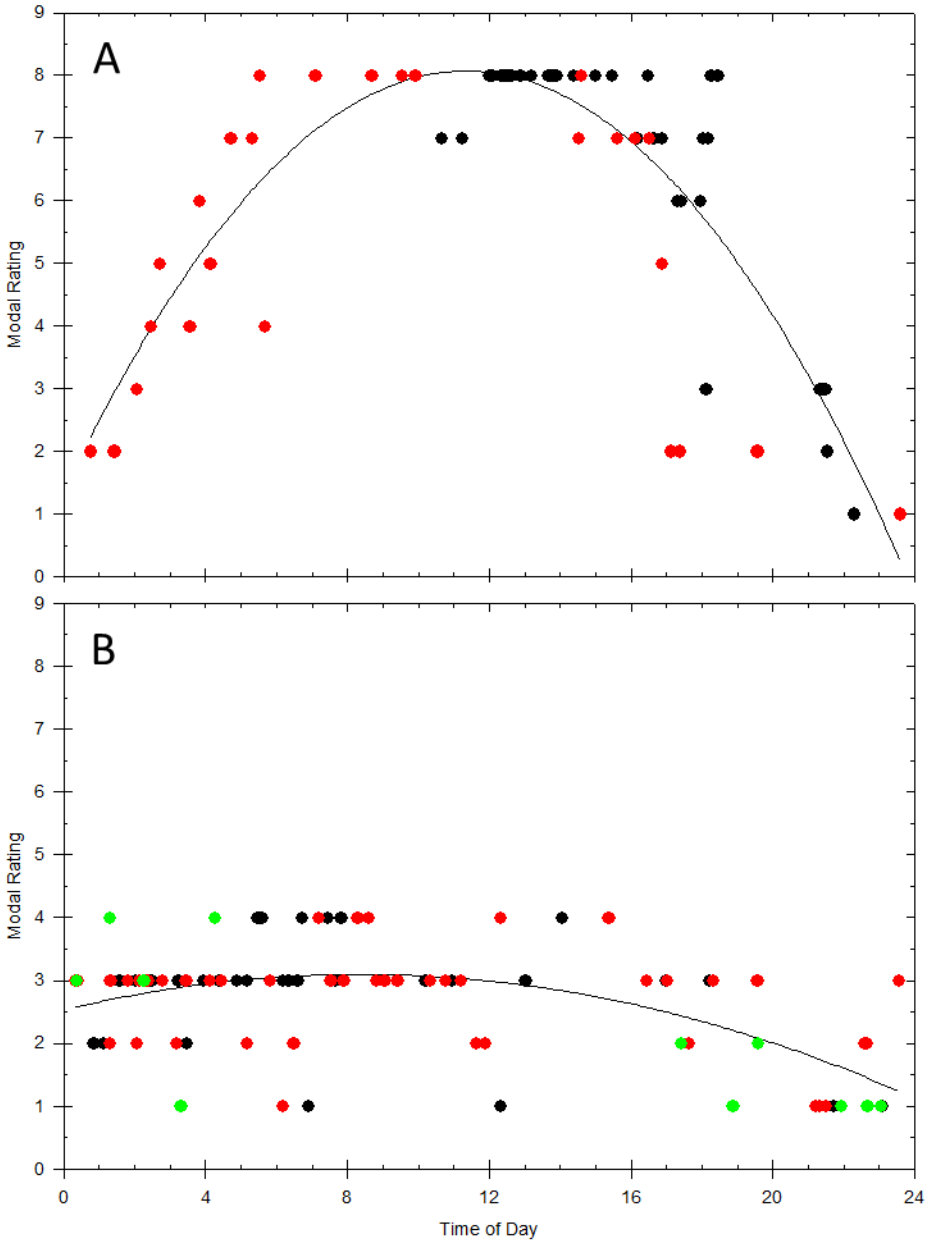

Figure 14 - Modal ratings with time of day for case type two days. a) Days where no precipitation occurred. Black circles are May 13 and red circles are May 25.b) Days where precipitation occurred. Black circles are May 14, red circles are May 23, and green circles are May 24.

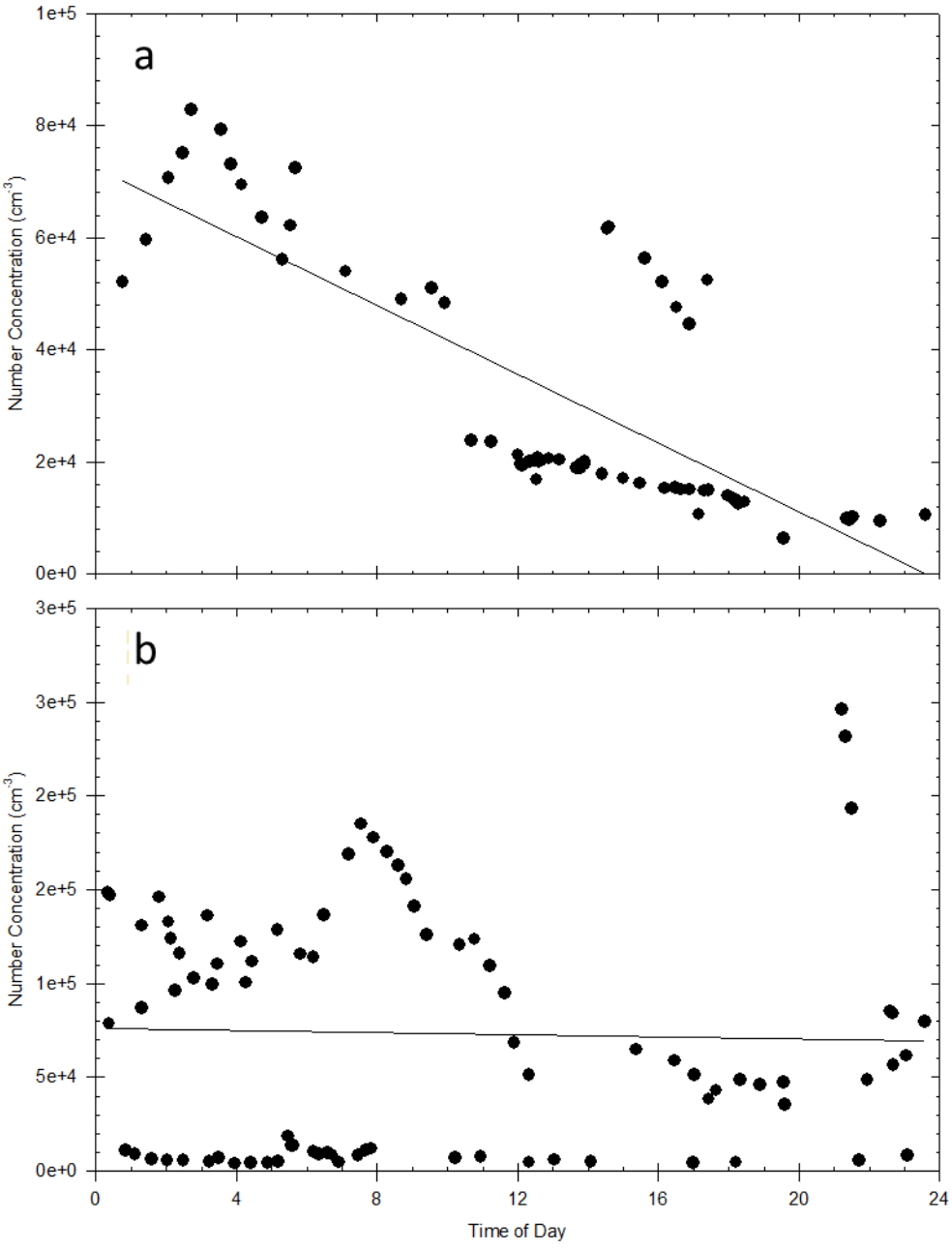

Figure 15 – N_{CCN} with time of day for case type two days. a) Days where no precipitation occurred. b) Days where precipitation occurred.

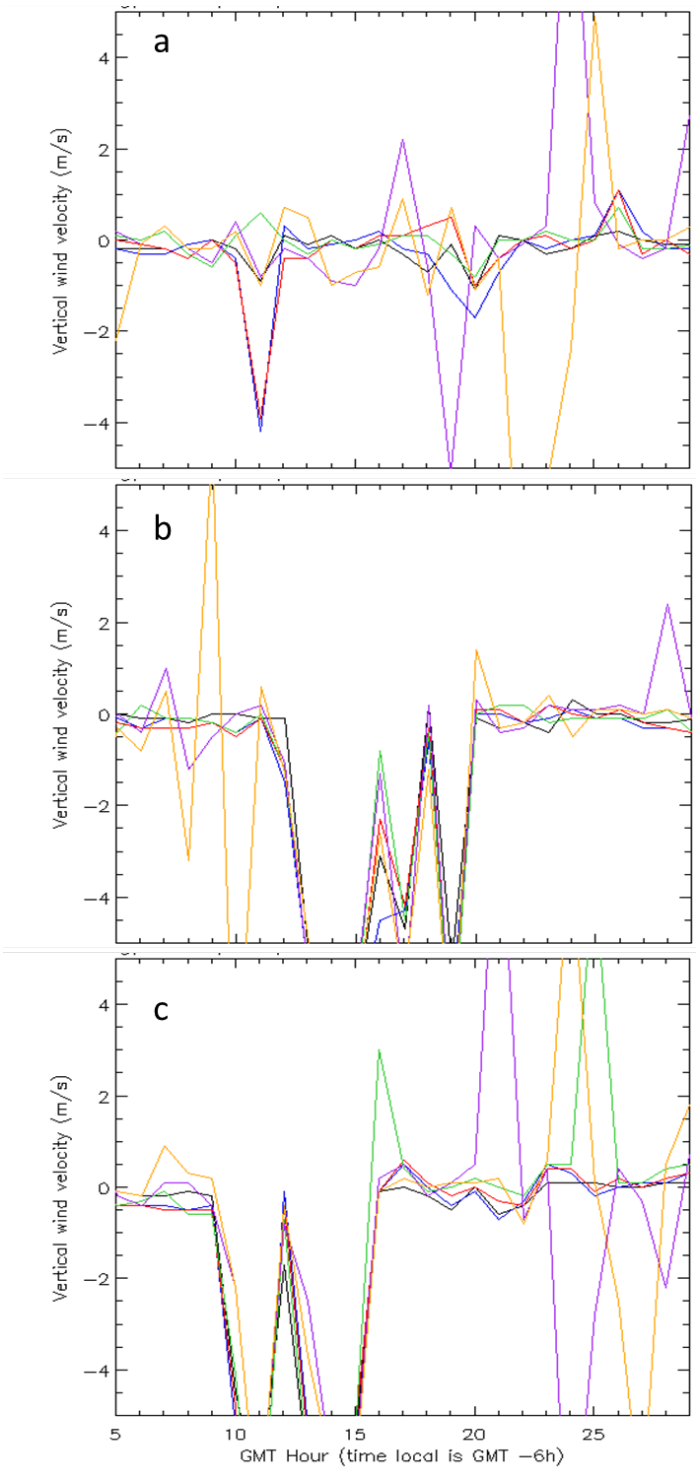

Figure 16 – Wind profiler derived vertical velocity for a) May 14, b) May 23, and c) 24. Each line represents a horizontal slice at a specified height above ground level, with 0.2km AGL (black), 0.5km AGL (blue), 0.7km AGL (red), 1.0 km AGL (green), 2.0 km AGL (purple), and 2.4km AGL (orange).

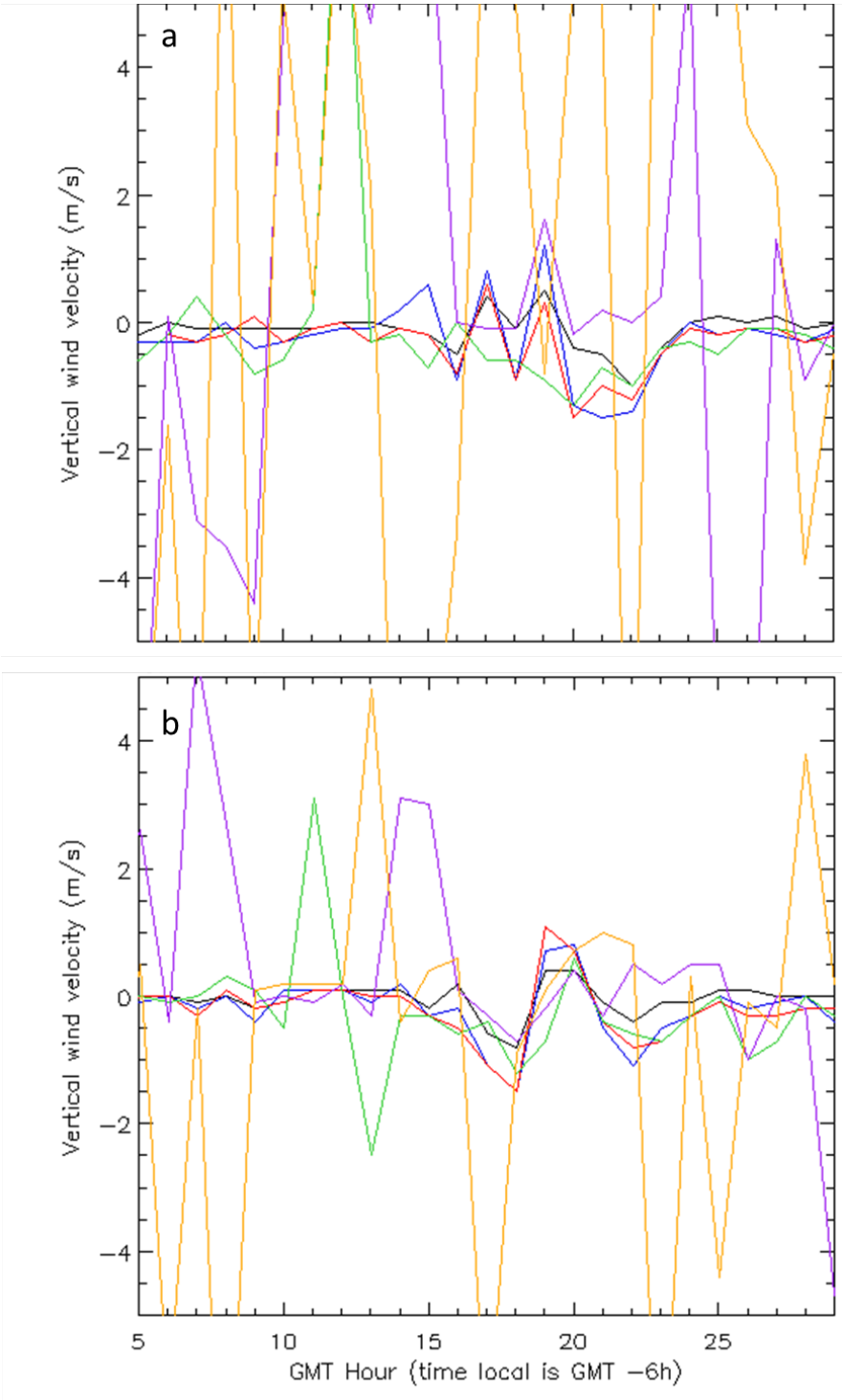

Figure 17 – Wind profiler derived vertical velocity for a) May 22 and b) May 26. Each line represents a horizontal slice at a specified height above ground level, with 0.2km AGL (black), 0.5km AGL (blue), 0.7km AGL (red), 1.0 km AGL (green), 2.0 km AGL (purple), and 2.4km AGL (orange).

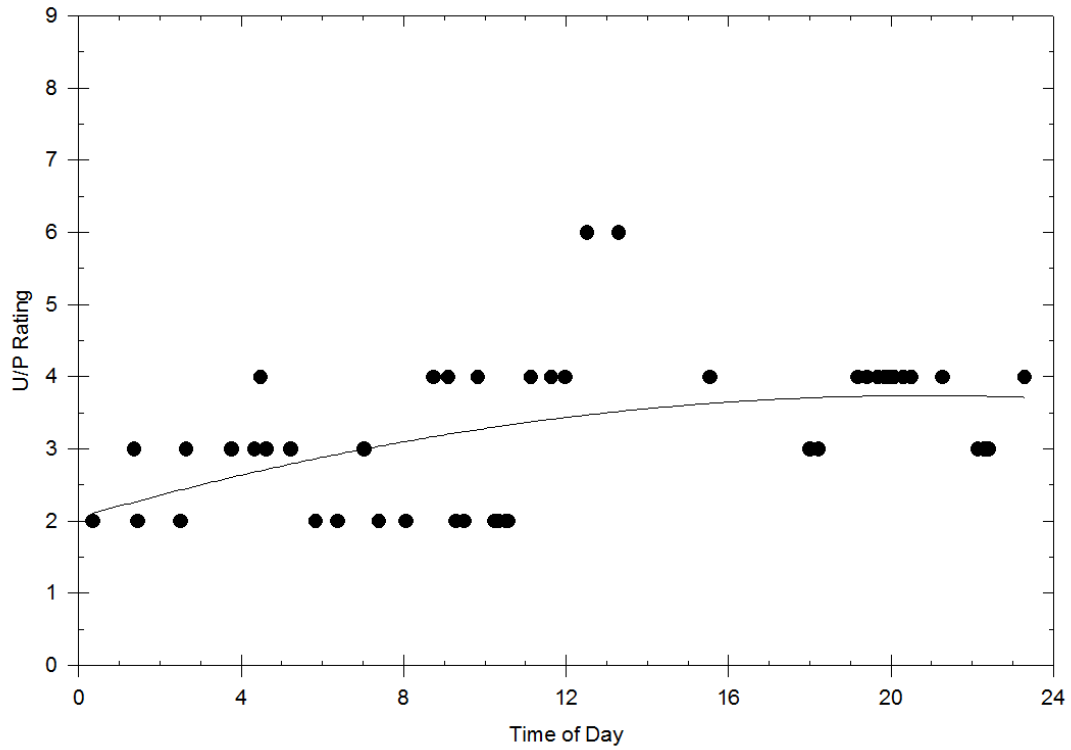

Figure 18 - U/P rating with time of day for case type three.

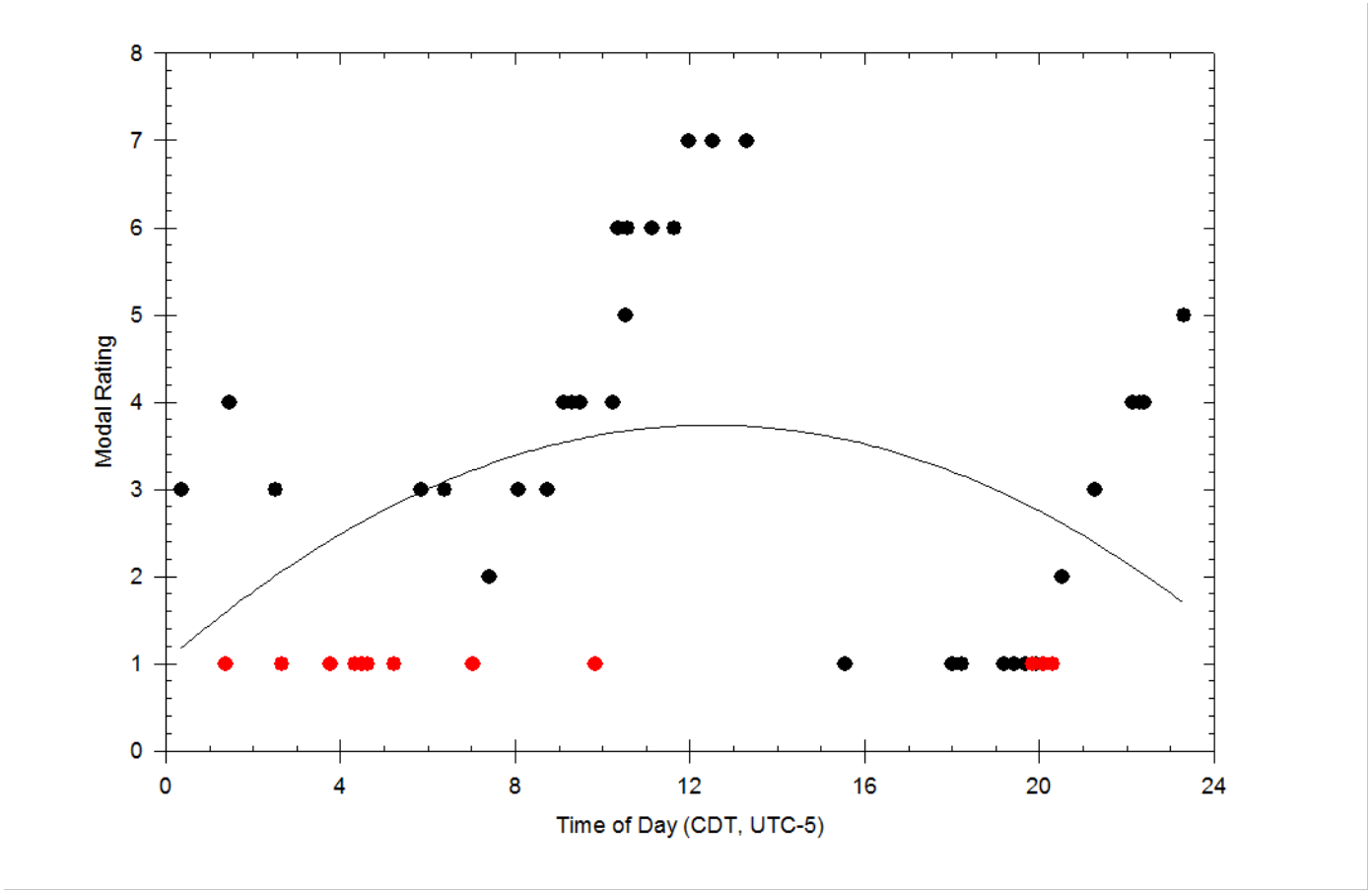

Figure 19 - Modal ratings with time of day for case type three days. Black circles are May 22 and red circles are May 26.

.

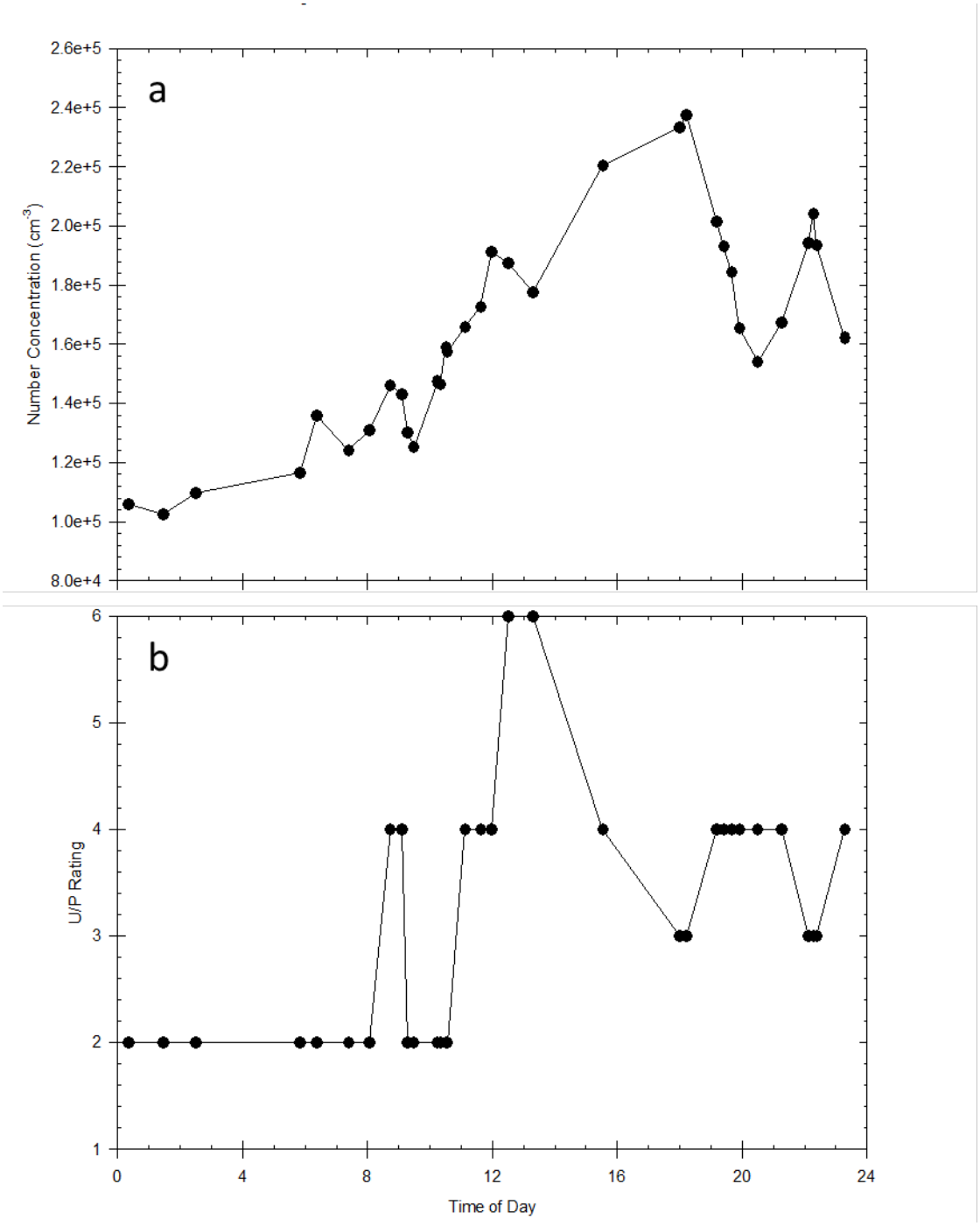

Figure 20- a) N_{CCN} with time for May 22. b) U/P rating with time for May 22.

.

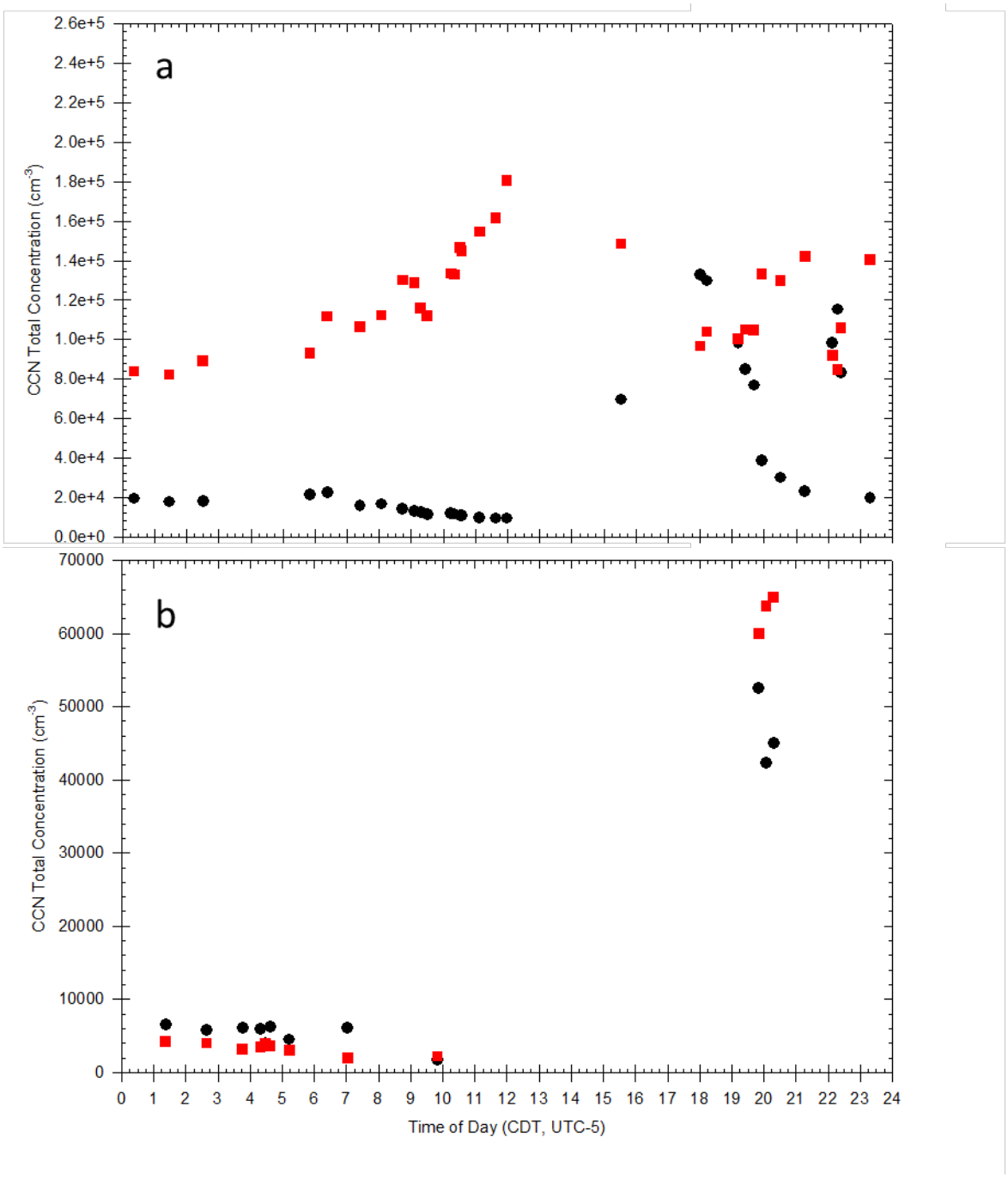

Figure 21- Unprocessed (black circles) and processed (red squares) N_{CCN} with time. a) May 22 b) May 26

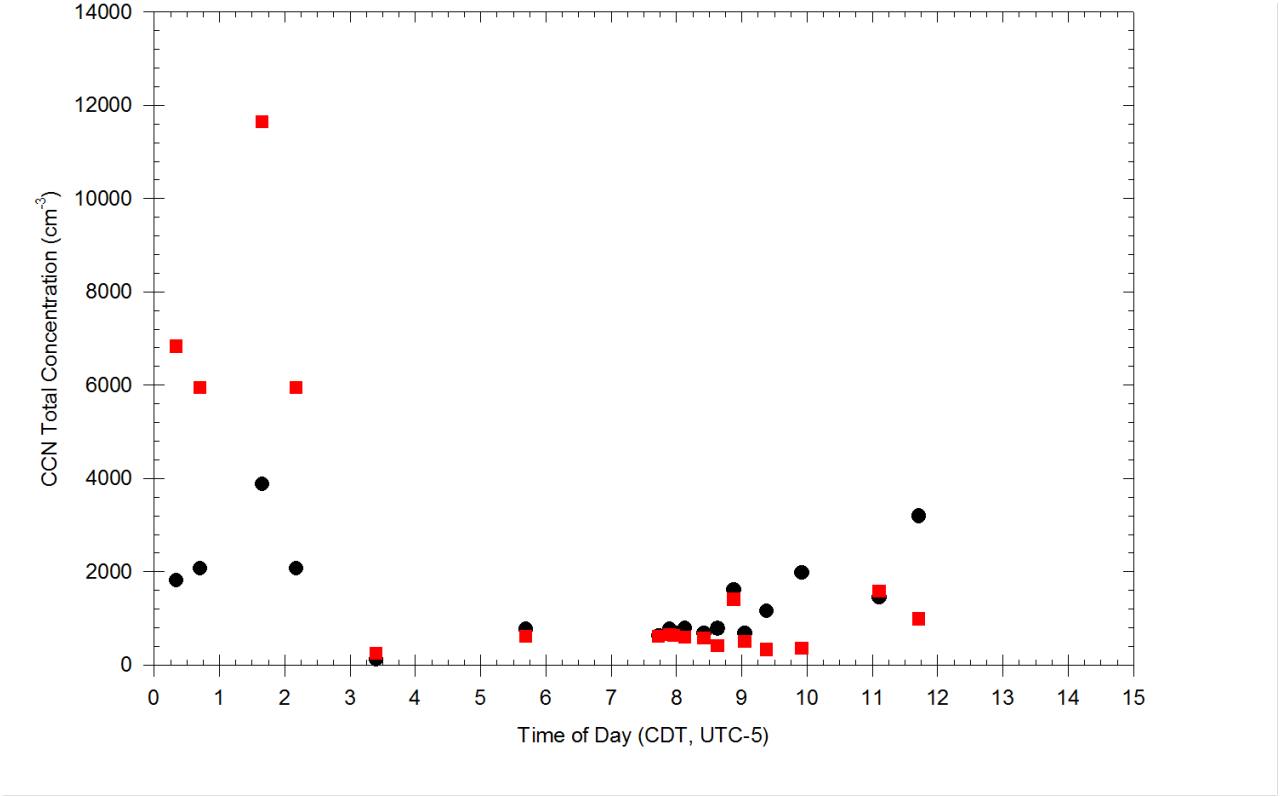

Figure 22 – Unprocessed (black circles) and processed (red squares) N_{CCN} for May 16.

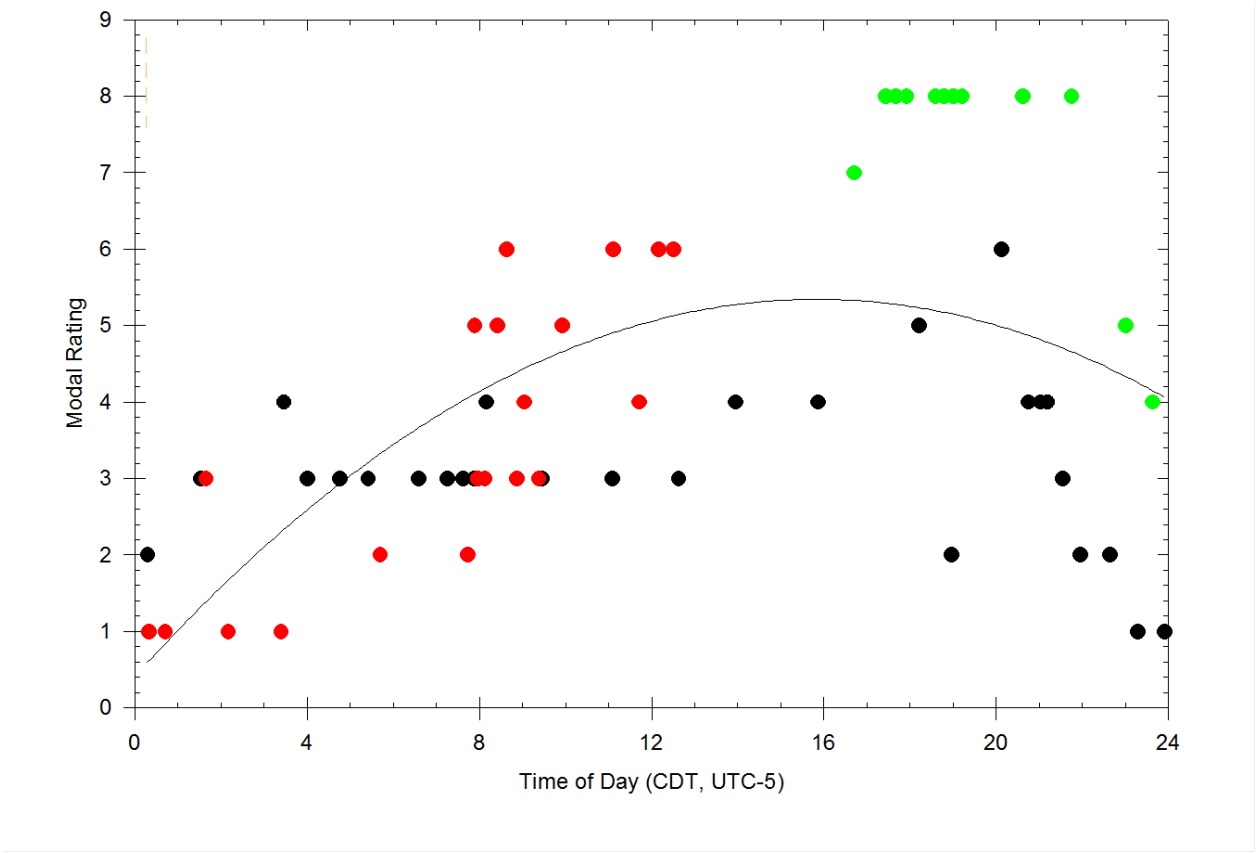

Figure 23 – Modal ratings with time for case type three. Black circles are May 15, red are May 16, and green are May 17.

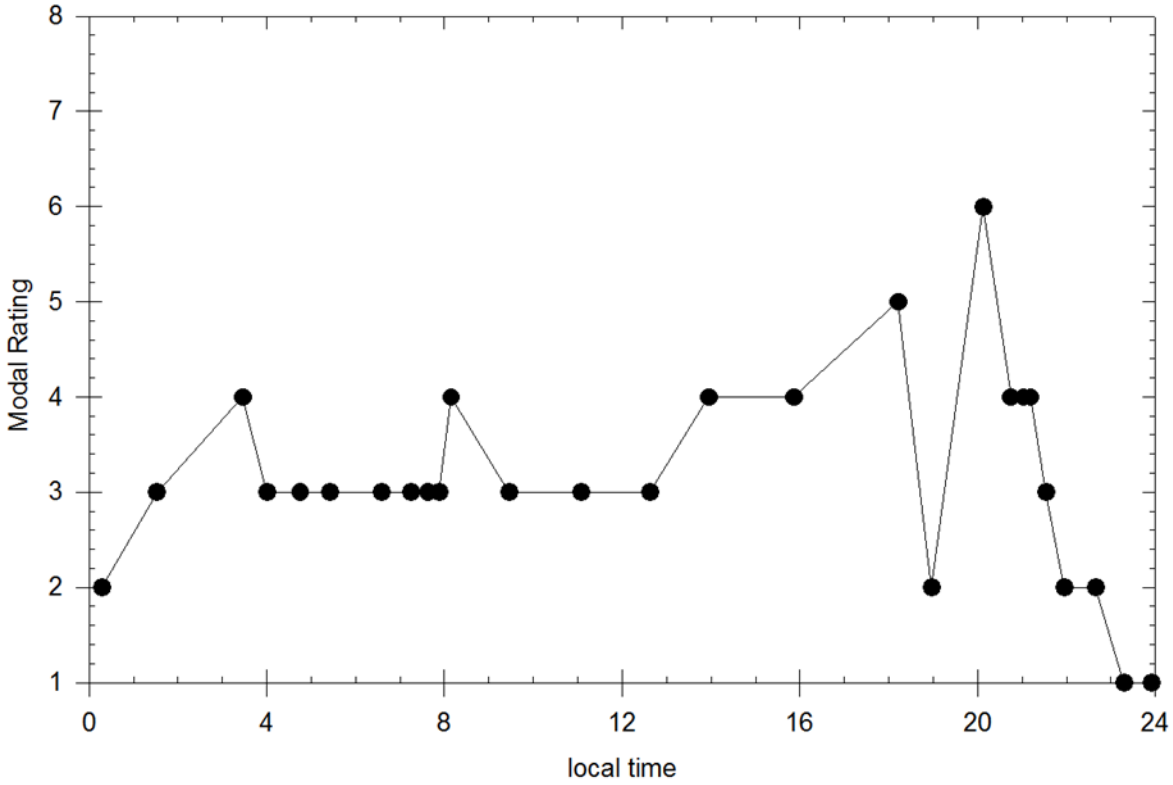

Figure 24 – Modal rating with time for May 15 (case type 4).

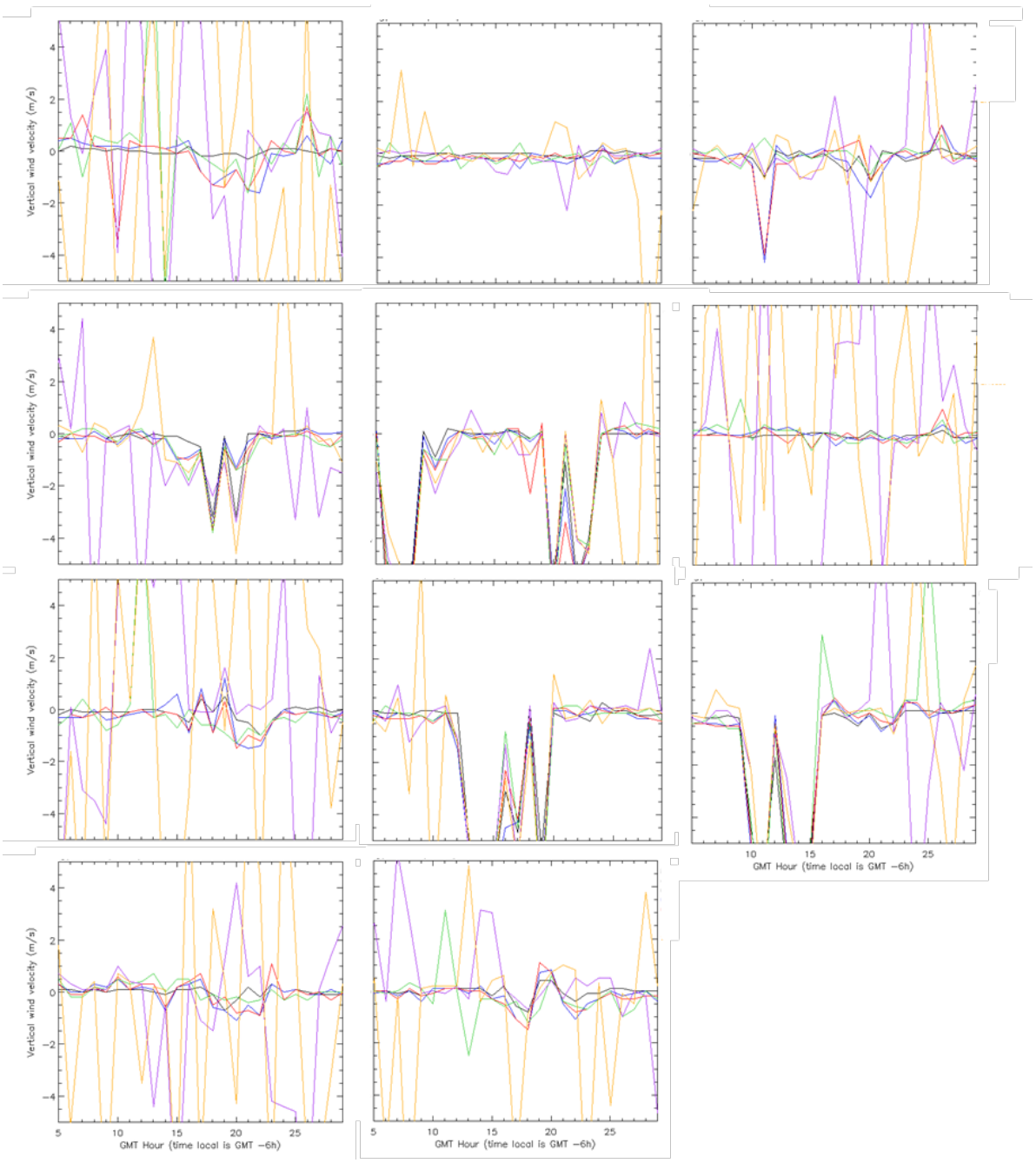

Figure 25 – Wind profiler derived horizontal sections of vertical velocity for each of the eleven case days. Left to right, top to bottom: May 11, May 13, May 14, May 15, May 16, May 17, May 22, May 23, May 24, May 25, May 26. Each line represents a horizontal slice at a specified height above ground level, with 0.2km AGL (black), 0.5km AGL (blue), 0.7km AGL (red), 1.0 km AGL (green), 2.0 km AGL (purple), and 2.4km AGL (orange).

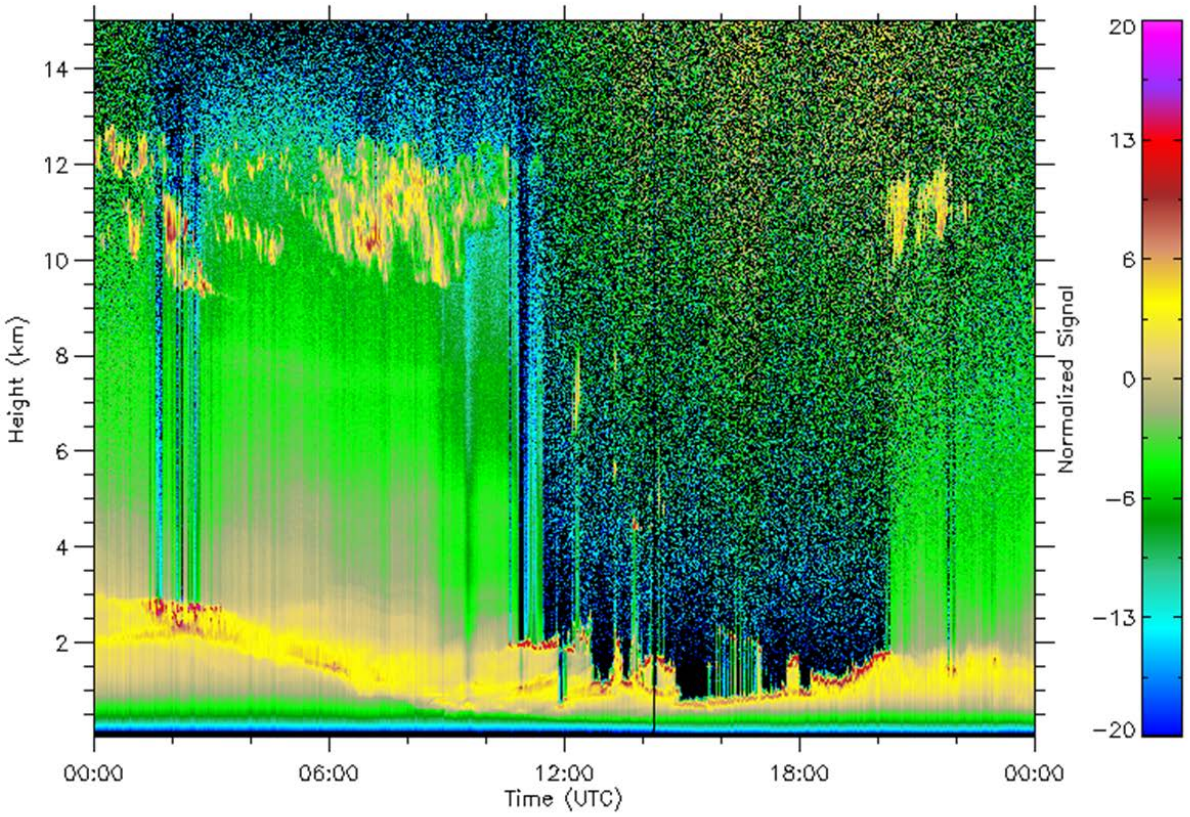

Figure 26 – LIDAR observations for May 13th from the ARM SGP central facility. Note that local time is UTC-5. The larger numbers represent a larger amount of signal being reflected back (such as by clouds) to the instrument.

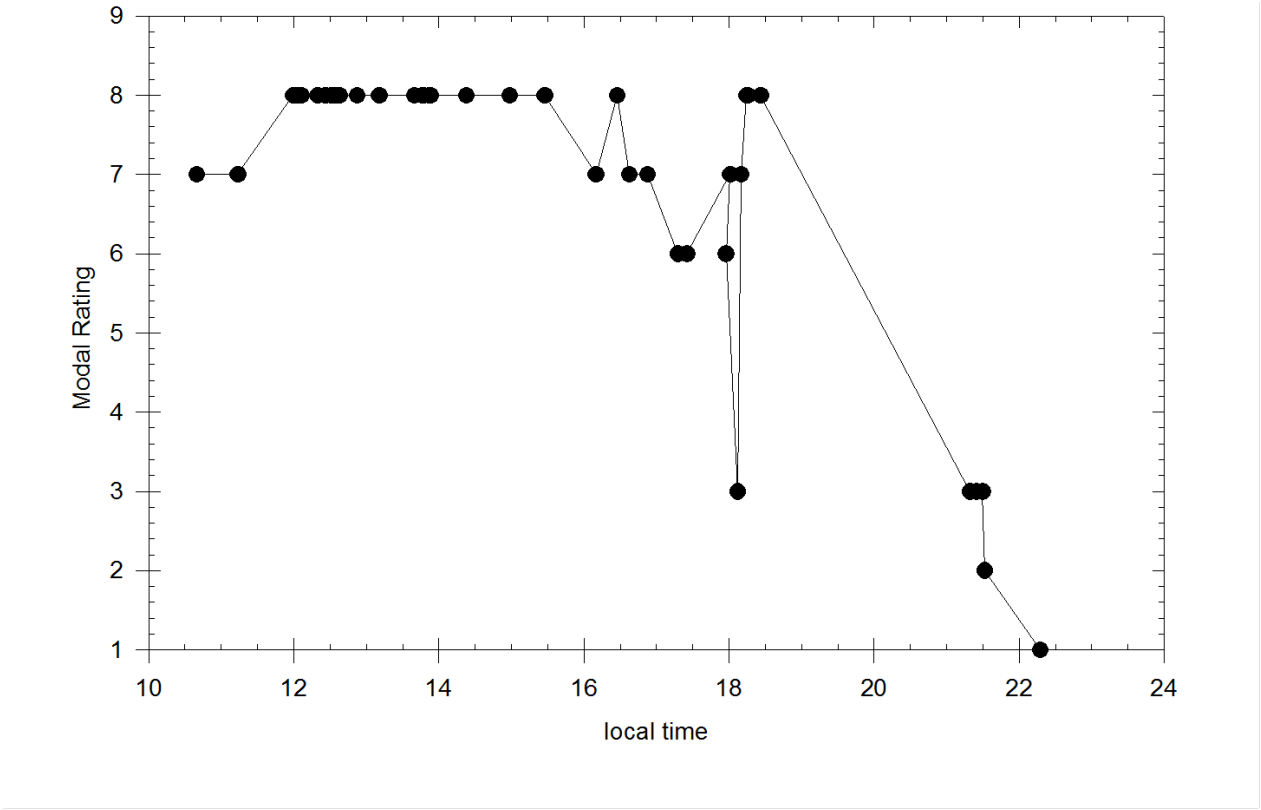

Figure 27 – Modal ratings with time for May 13. Local time is UTC-5.

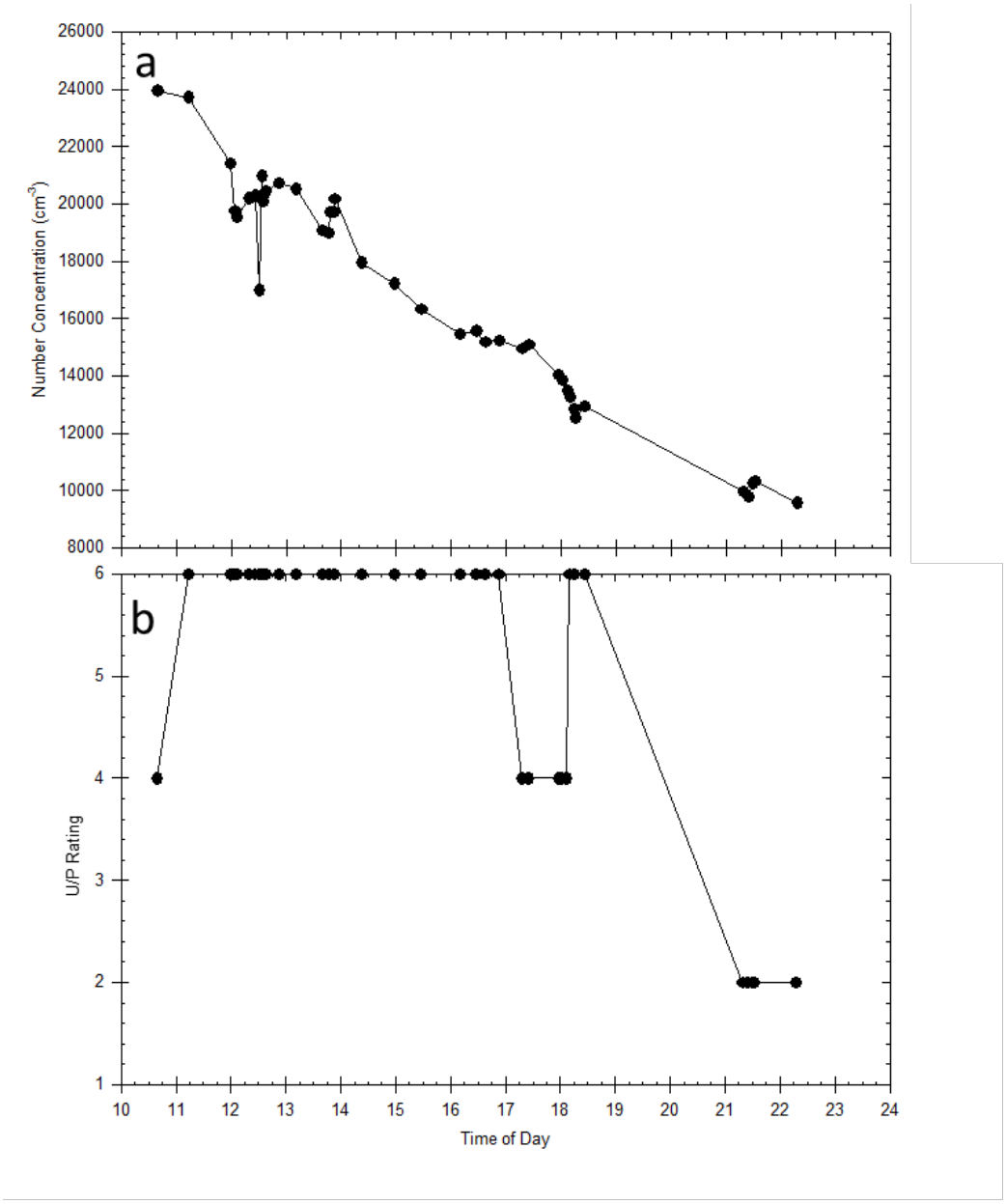

Figure 28 - a) N_{CCN} with time for May 13. b) U/P rating with time for May 13.

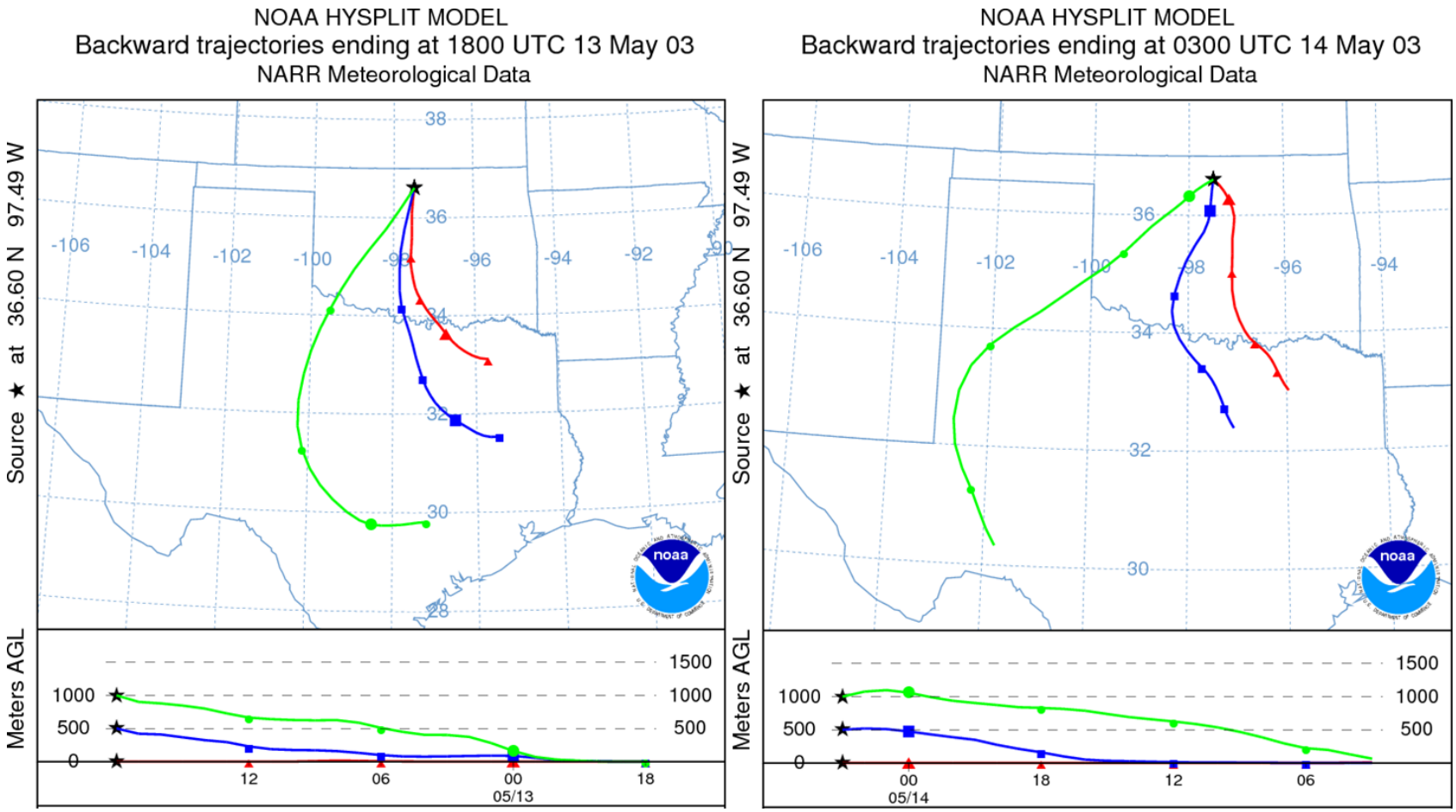

Figure 29– HY-SPLIT back trajectory analysis for May 13. a) Run beginning at 1800 UTC (1300 CDT). b) Run beginning at 0300 UCT May 14 (2200 CDT May 13).

Works Cited

Albrecht, B. A. (1989), Aerosols, cloud microphysics, and fractional cloudiness, *Science, 245*, 1227-1230.

Alexander, L. V. and Coauthors (2013), Summary for Policymakers. Climate Change 2013: The Physical Science Basis, Stocker T. F. et al., Cambridge University Press, 1-29.

Bougiatioti, A., Nenes, A., Fountoukis, C., Kalivitis, N., Pandis, S., & Mihalopoulos, N. (2011). Size-resolved CCN distributions and activation kinetics of aged continental and marine aerosol. *Atmos. Chem. Phys. Discuss. Atmospheric Chemistry and Physics Discussions*, 12607-12648.

Carslaw, K., Lee, L., Reddington, C., Pringle, K., Rap, A., Forster, P., . . . Pierce, J. (2013). Large contribution of natural aerosols to uncertainty in indirect forcing. Nature, 67-71.

Clarke, A. D., F. Eisele, V. N. Kapustin, K. Moore, D. Tanner, L. Mauldin, M. Litchy, B. Lienert, M. A. Carroll, and G. Albercook (1999), Nucleation in the equatorial free troposphere: Favorable environments during PEM-Tropics, *J. Geophy. Res., 104(D5)*, 5735–5744, doi:10.1029/98JD02303.

Clarke, A.D., S. Freitag, R. Simpson, J.G. Hudson, S. Howell, V. Brekhovskikh, T. Campos, V. Kapustin (2013), Free troposphere as the dominant source of CCN in the equatorial Pacific boundary layer: Long-range transport and teleconnections, *Atmos. Chem. Phys. 13* (15):7511-7529.

Clarke, A. D., Z. Li, M. Litchy (1996), Aerosol dynamics in the equatorial Pacific marine boundary layer: Microphysics, diurnal cycles and entrainment, *J. of Geophy. Res., 23(8)*, 733-736, doi:10.1029/96GL00778.

Clarke, A. D., Y. Shinozuka, V.N. Kapustin, S. Howell, B. Huebert, S. Doherty, T. Anderson, D. Covert, J. Anderson, X. Hua, K.G. Moore II, C. McNaughton, G. Carmichael, and R. Weber (2004), Size distributions and mixtures of dust and black carbon aerosol in Asian outflow: Physiochemistry and optical properties, *J. Geophy. Res.*, *109*, D15S09, doi:10.1029/2003JD004378.

Clarke, A. D., J. L. Varner, F. Eisele, R. L. Mauldin, D. Tanner, and M. Litchy (1998), Particle production in the remote marine atmosphere: Cloud outflow and subsidence during ACE 1, *J. Geophy. Res.*, *103(D13)*, *16397–16409*, doi:10.1029/97JD02987.

Dusek, U., Frank, G., Curtius, J., Drewnick, F., Schneider, J., Kürten, A., . . . Pöschl, U. (2009). Enhanced organic mass fraction and decreased hygroscopicity of cloud condensation nuclei (CCN) during new particle formation events. *Geophys. Res. Lett.*

Feingold, G., Kreidenweis, S., Stevens, B., & Cotton, W. (1996). Numerical simulations of stratocumulus processing of cloud condensation nuclei through collision-coalescence. *J. Geophys. Res.*, 21391-21391.

Feingold, G., Kreidenweis, S., & Zhang, Y. (1998). Stratocumulus processing of gases and cloud condensation nuclei: 1. Trajectory ensemble model. *J. Geophys. Res.*, 19527-19527.

Feingold, G., & Kreidenweis, S. (2000). Does cloud processing of aerosol enhance droplet concentrations? *J. Geophys. Res.*, 24351-24361.

Gerber, H. E., Hoppel, W. A., and Wojciechowski, T. A. (1997). Experimental verfications of the theoretical relationship between size and critical supersaturation of salt nuclei. *J. Atmos. Sci.*, 34, 1410-1420.

Holmgren, H., Sellegri, K., Hervo, M., Rose, C., Freney, E., Villani, P., & Laj, P. (2014). Hygroscopic properties and mixing state of aerosol measured at the high altitude site Puy de Dôme (1465 m a.s.l.), France. Atmos. Chem. Phys. Discuss. *Atmospheric Chemistry and Physics Discussions*, 6759-6802.

Hoppel, W., Fitzgerald, J., & Larson, R. (1985). Aerosol size distributions in air masses advecting off the east coast of the United States. *J. Geophys. Res*., 2365-2365.

Hoppel, W., Frick, G., & Larson, R. (1986). Effect of nonprecipitating clouds on the aerosol size distribution in the marine boundary layer. *Geophys. Res. Lett.*, 125-125.

Hoppel, W., Fitzgerald, J., Frick, G., Larson, R., & Mack, E. (1990). Aerosol Size Distributions and Optical Properties Found in the Marine Boundary Layer over the Atlantic Ocean. *J. Geophys. Res.*, 3659-3686.

Hoppel, W., Frick, G., Fitzgerald, J., & Larson, R. (1994). Marine boundary layer measurements of new particle formation and the effects nonprecipitating clouds have on aerosol size distribution. *J. Geophys. Res.*, 14443-14459.

Hoppel, W., Frick, G., & Fitzgerald, J. (1996). Deducing droplet concentration and supersaturation in marine boundary layer clouds from surface aerosol measurements. *J. Geophys. Res.*, 26553-26565.

Hudson, J. and Noble, S. (2014a), CCN and vertical velocity influences on droplet concentrations and supersaturations in clean and polluted stratus clouds, *J. Atms. Sci.*

Hudson, J., & Noble, S. (2014b). Low altitude Summer/Winter microphysics, dynamics and CCN spectra of Northeastern Caribbean small cumuli; and comparisons with stratus. *J. Geophys. Res. - Atmos*., 5445-5463.

Hudson, J. G., Noble, S. R., Tabor, S. S. (2015). Cloud supersaturations from CCN spectra Hoppel minima, *J. Geophys. Res. - Atmos*., March 18, 2015, Accepted

Hudson, J. (1989). An Instantaneous CCN Spectrometer. *Journal of Atmospheric and Oceanic Technology,* 1055-1065.

Hudson, J. (1982). Effects of CCN Concentrations on Stratus Clouds. *J. Atmos. Sci.,* 480-486.

Hudson, J. (2007). Variability of the relationship between particle size and cloud-nucleating ability. *Geophysical Research Letters*.

Petters, M., & Kreidenweis, S. (2007). A single parameter representation of hygroscopic growth and cloud condensation nucleus activity. *Atmospheric Chemistry and Physics Discussions,* 8435-8456.

Platnick, S., & Twomey, S. (1994). Determining the Susceptibility of Cloud Albedo to Changes in Droplet Concentration with the Advanced Very High Resolution Radiometer. *J. Appl. Meteor*., 334-347.

Pruppacher H.R. and Klett, J. D. (1978). Microphysics of clouds and precipitation. D. Reidel, Hinghman, Mass., 714.

Raatikainen, T., A. Nenes, J.H. Seinfeld, R. Morales, R.H. Moore, T.L. Lathem, S. Lance, L.T. Padro, J.J. Lin, K.M. Cerully, A. Bougiatioti, J. Cozic, C.R. Ruehl, P.Y. Chuang, B.E. Anderson, R.C. Flagan, H. Jonsson, N. Mihalopoulos, and J.N. Smith (2013), Worldwide data sets constrain the water vapor uptake coefficient in cloud formation, *PNAS, 10*, 10 3760-3764, doi:10.1073/pnas.1219591110

Roberts, G., Andreae, M., Zhou, J., & Artaxo, P. (2001). Cloud condensation nuclei in the Amazon Basin: “marine” conditions over a continent? *Geophysical Research Letters Geophys. Res. Lett.*, 2807-2810.

Svenningsson, B., Hansson, H., Martinsson, B., Wiedensohler, A., Swietlicki, E., Cederfelt, S., . . . Colvile, R. (1997). Cloud droplet nucleation scavenging in relation to the size and hygroscopic behaviour of aerosol particles. *Atmospheric Environment*, 2463-2475.

Swietlicki, E., Zhou, J., Berg, O., Martinsson, B., Frank, G., Cederfelt, S., . . . Bower, K. (1999). A closure study of sub-micrometer aerosol particle hygroscopic behaviour. *Atmospheric Research*, 205-240.

Twomey, S. (1974). Pollution and the Planetary Albedo. *Atmospheric Environment*, 120-125.

Twomey, S. (1977). The Influence of Pollution on the Shortwave Albedo of Clouds. *J. Atmos. Sci.*, 1149-1152.

Wang, J., Daum, P., Kleinman, L., Lee, Y., Schwartz, S., Springston, S., . . . Elleman, R. (2007). Observation of ambient aerosol particle growth due to in-cloud processes within boundary layers. *J. Geophys. Res. Journal of Geophysical Research*.

Wang, J., Flagan, R., & Seinfeld, J. (2003). A Differential Mobility Analyzer (DMA) System for Submicron Aerosol Measurements at Ambient Relative Humidity. *Aerosol Science and Technology*, 46-52

Yakobi-Hancock, J., Ladino, L., Bertram, A., Huffman, J., Jones, K., Leaitch, W., . . . Abbatt, J. (2014). CCN activity of size-selected aerosol at a Pacific coastal location. *Atmos. Chem. Phys.*, 12307-12317.

Zhang, Y., Kreidenweis, S., & Feingold, G. (1999). Stratocumulus processing of gases and cloud condensation nuclei: 2. Chemistry sensitivity analysis. *J. Geophys. Res.*, 16061-16061.

Zhou, J., Swietlicki, E., Hansson, H., & Artaxo, P. (2002). Submicrometer aerosol particle size distribution and hygroscopic growth measured in the Amazon rain forest during the wet season. *J. Geophys. Res.*, 8055.